Physics – Uspekhi **38** (6) 567 – 591 (1995)

REVIEWS OF TOPICAL PROBLEMS PACS numbers: 79.90.+b

Ecton or electron avalanche from metal

G A Mesyats

Contents

Abstract. The so-called explosive electron emission observed as individual packets or avalanches of electrons is shown to occur in microexplosions at the cathode. This microexplosion of electrons is called an ecton. Electron current in an ecton starts to flow as a result of the overheating of metal because of the high energy density (10^4 J g^{-1}), and the current stops owing to the cooling of the emission zone. Ectons occur in electrical discharges in vacuum, in cathode spots of a vacuum arc, in bulk discharges in gases, in pseudo-spark discharges, in corona discharges, etc.

1. Introduction

Electron emission from a metal occurs typically when an electron acquires an additional energy from an outer source or when the tunneling is provided for. In this review it is shown how short-time avalanches and electron packets occur under conditions suitable for an emission which electrons themselves ensure. For this, microexplosions at the cathode are responsible. They are provoked by a high-energy concentration and strong overheating of the metal. I call these avalanches of charged particles 'ectons' [1], after the first letters of the expression 'explosive centre'. The ecton owes its discovery to studies of explosive electron emission (EEE) [4].

The explosive electron emission is the electron current from a conductor, which is a cathode, as a result of the explosion of a microscopic volume on its surface. The explosion of a microvolume of metal and excitation of EEE occur for various reasons, including the impact of a highly accelerated bit of material on the cathode, or the exposure of the cathode to a power pulse of laser radiation or a beam of charged or neutral particles.

However, the most common way of exciting EEE is rapid heating of microportions of the cathode by an electric current of high density. The simplest example is the current of field emission (FE) from cathode micropeaks, the density of which reaches 10^9 A cm^{-2} and more for intensive electric fields. It has long been believed that only the FE current could excite the EEE. Now it is clear that some other processes can also excite the EEE.

The author and his collaborators have conducted systematic studies on the mechanism of this phenomenon since the 1960s. The studies met with success in 1966 [2] when it was established, by observations of cathode – anode processes in vacuum for the pulse electric field of an average strength 10^6 W cm^{-1} and for the time resolution up to 10^{10} s, that an electron current occurs as the result of explosions of micropoints at the cathode under the action of

G A Mesyats Institute of Electrophysics, Russian Academy of Sciences
ul. Pervomaiskaya 91, 620219 Ekaterinburg, Russia
Tel. (3432) 44 02 23, Fax (3432) 44 41 33
E-mail: romanov@mik.e-burg.su

Received 7 February 1995
Uspekhi Fizicheskikh Nauk **165** (6) 601–626 (1995)
Translated by D Kh Gan'zha; edited by L Dwivedi

the FE current and the strength of the resultant current exceeds that of the initial current by several orders of magnitude.

In Ref. [3] the following conclusions are made: "the surface of a cathode is not ideal, it is rough"; "peaks on the cathode are sources of FE since the field is locally intensified there"; "separate bright spots can be associated with explosions of peaks"; "the glow at the cathode is caused by processes triggered by the electron beam, which is drawn from the plasma derived from the evaporated material of the cathode". Thus, it outlined the range of phenomena which are now called the explosive electron emission. In later works, the EEE conception was formulated in the current form.

An ecton is accompanied by a series of very complicated phenomena (plasma, melting of microparts at the cathode, splashing of metallic droplets, etc.). For these processes, the high density of plasma (over 10^{20} cm^{-3}) in the cathode part of the emission zone, strong inhomogeneity of plasma in small volumes (10^{12} cm^{-3}), short durations of processes ($10^{-10}-10^{-8}$ s), high current density at the anode, and so on, are typical.

In an ecton, electrons are emitted for $10^{-9}-10^{-8}$ s and then the emission stops on its own since the explosive centre cools down because of the heat conduction, decrease in the current density, and slopping of metal. The energy concentration in a microvolume of the cathode must be greater than the energy of sublimation (over 10^4 J g^{-1}) at a total energy of 10^{-8} J, for an ecton to be excited. The ecton superficially has much in common with an electron avalanche in gas. In either case, electrons are produced in abundance for a short time. The difference is that, in an ecton, electrons are emitted from the cathode, and in an electron avalanche they are generated by ionised multiplication. In either case, the growth of the number of electrons starts to decelerate on its own within a short time ($10^{-9}-10^{-8}$ s). In an ecton, the reason is the cooling of the emission zone, and in an avalanche in gas the reason is the growth of the field of the positive space charge of ions which drastically decreases the impact ionisation coefficient.

The explosive electron emission plays a fundamental role in vacuum sparks and arcs, in low-pressure discharges, in compressed and high-strength gases, in microgaps etc., that is, when there is a high electric field at the cathode. The discovery and thorough investigation of FE and ectons, and also advances in powerful nanosecond pulse equipment made it possible to create pulse electron accelerators with powers up to 10^{13} W and more for pulse duration $10^{-10}-10^{-6}$ s, electron current $1-10^6$ A, and energy of electrons 10^4-10^7 eV. Such beams are widely accepted for investigations in plasma physics, radiative physics, and chemistry; in technology, for gas laser pumping, generation of high-power UHF and x-ray pulses, etc. I am sure that ectons underlie such processes as the electric-spark working of metal, electric-spark doping, processes on contacts, in switching equipment, etc.

What are the facts that prove the existence of an ecton? These facts were obtained from studies of explosive electron emission, vacuum discharges, and vacuum arcs (see Section 6.1.3). The first most important evidence of the existence of ectons is craters at the cathode [9] (Fig. 1). Since a crater is formed with a finite velocity (between the velocity of heat conduction and the velocity of sound),

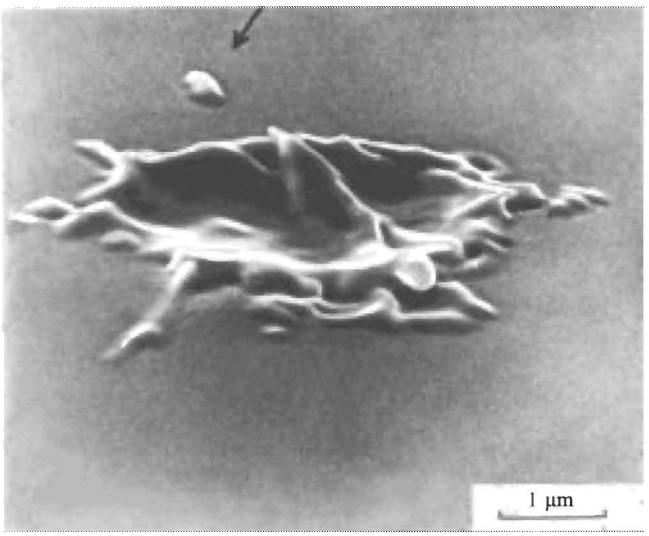

Figure 1. A crater at a molybdenum cathode. It was produced by an ecton for 10 ns.

$v_{cr} \approx 10^4-10^5$ cm s^{-1}, given the radius of the crater r_{cr} the lifetime of an ecton can be estimated as $t_e \sim r_{cr}/v_{cr}$. Usually $r_{cr} \sim 10^{-4}$ cm, therefore, $t_e \sim 10^{-9}-10^{-8}$ s.

The second argument in favour of the existence of ectons is the time structure of the vacuum discharge current. If, for example, there is a point cathode and a plane anode, then the current builds up smoothly in vacuum discharge. However, if the anode is punctured opposite the point, then the current will increase 2–3 times behind the opening for short times, in comparison with the mean current. The duration of beams generated will be $10^{-9}-10^{-8}$ s [4]. This means that charged particles appear and disappear at the cathode.

The third important argument in favour of ectons is that many specific parameters are independent of the discharge current. For example, the velocity of scattering of plasma is independent of the current until the pinch effect is triggered [4–6]. The specific force (force per unit current) the cathode experiences in a vacuum arc is independent of the current [6]. The number of droplets per unit charge the cathode emits in a vacuum arc is also independent of the current [7]. Finally, there exists a limit for the specific mass carried away from the cathode in a vacuum arc, which depends only on the material out of which the cathode is made and is independent of the current. The mass is carried away as positive ions moving against the electric field from the cathode to the anode [8]. The model proposed explains all these facts.

2. Electric explosion of metal and ectons

2.1 Electric explosion of conductors

When it comes to ectons, it is assumed that what occurs in the microvolume of metal is approximately the same as in the electric explosion of a conductor (EEC) [10]. Of interest for the physics of EEC is the rapid heating of conductors with the rate 10^{12} K s^{-1}. This makes it possible to study physical properties of metals and their phase changes in rapid transitions through all states of matter — from a solid state to plasma. Such studies are important for understanding the properties of metals regarding the critical

point of nonideal plasma and also the high-temperature metal–nonmetal phase transition [11].

The EEC process may be divided into two stages. The initial stage involves the heating of metal in the solid state, melting, and heating of metal up to a point at which it starts to evaporate. At this stage, the metal density changes but only slightly. Then the explosion itself occurs. It is accompanied by an abrupt increase in the resistance of the conductor by a factor of 10^2 or more. The reason is the expansion and, consequently, the decrease in the density of the conductor. The change in the metal density essentially affects the electron spectrum of the metal and mechanisms of its electric conduction. For example, the specific resistance increases 10 times as the copper density decreases 2 times [10]. The specific resistance κ increases 10^3 times in comparison with that in the normal state, when the specific energy $w \sim 10^4$ J g^{-1} is delivered to a copper conductor [10].

At the initial state of EEC, the physical state of the metal can be described by one thermodynamic variable: temperature or specific energy. For example, the formula

$$\kappa = \kappa_1(1 + \beta_s w) \tag{2.1}$$

is true for the specific resistance of a solid conductor [10]. Here κ_1 is the initial specific resistance, w is the specific energy, and β_s is the energy coefficient of resistance in the solid state. For example, $\beta_s = 5.3 \times 10^{-3}$ g kJ^{-1} for Al and $\beta_s = 6.8 \times 10^{-3}$ g kJ^{-1} for Cu. The dependence $\kappa(w)$ is approximated by another formula for the metal in a liquid state up to the point at which the resistance starts to increase abruptly [10]:

$$\kappa = \kappa_{1l}\left[1 + \beta_l(w - w_{0l})\right] , \tag{2.2}$$

where κ_{1l} is the initial specific resistance of a liquid metal; β_l is a factor; w_{0l} is the specific internal energy at the melting point.

The stage of the explosion itself is not so clear. At this stage there are a series of phenomena which complicate the physical pattern of EEC. These phenomena refer to instability, shunting discharges, stratoformations, etc. One of the peculiar features of this stage is that the ohmic resistance is not unique for the specific energy delivered and depends on the specific power [12].

Besides experimental research, there are three more research approaches to EEC: numerical simulation, simplified calculations based on models, and similarity methods. In calculating EEC by a similarity method, of importance is the specific action integral (the specific action):

$$\bar{h} = \int_0^{t_d} j^2 \, dt ,$$

where j is the current density and t_d is the explosion delay time.

This quantity remains constant for many metals on change in the current density by a factor of 10 or more. This fact can readily be explained. If the diameter of a circular conductor d is much less than its length l ($d \ll l$), then the specific energy released in the EEC is

$$\int_0^{t_d} j^2 \kappa(w) \, dt = w\rho , \tag{2.3}$$

Table 1.

Metal	Al	Ag	Au	Cu	Ni	Fe	W
$\bar{h}/10^9$ A^2 s cm^{-4}	0.9	1	1	2	0.8	0.6	0.8

where ρ is the density of metal. Considering Eqns (2.1) and (2.2), Eqn (2.3) can be written in the form

$$\int_0^{t_d} j^2 \, dt = \int_{w_0}^{w_{ex}} \frac{\rho}{w\kappa(w)} \, dw , \tag{2.4}$$

where w_0 is the initial specific energy, and w_{ex} is the specific energy in the explosion.

The quantity on the right-hand side of formula (2.4) is the specific action. In Table 1 experimental data are listed for the specific action $\bar{h}$ of various conductors at the initial room temperature provided that the largest current density is 10^7 A cm^{-2} [13].

That $\bar{h}$ depends but weakly on t and j for $j \leqslant 10^7$ A cm^{-2} is shown in several other works. Some of them are reviewed in Ref. [17]. The increase in the current density to 10^8A cm^{-2} or more results in an increase of the specific action. For example, $\bar{h} \approx 4 \times 10^9$ A^2 s cm^{-4} for copper when $j \geqslant 10^8$ A cm^{-2} [13].

Sometimes the classical approach is used for coarse evaluations of the specific action: the explosion is supposed to occur when a critical temperature T_{ex} is reached. Given that

$$\bar{h} = \rho \int_{T_0}^{T_{ex}} \frac{c}{\kappa} \, dT ,$$

and $\kappa = \kappa_0 T$, then

$$\int_0^{t_d} j^2 \, dt = \frac{\rho c}{\kappa_0} \ln \frac{T_{ex}}{T_0} = \bar{h} , \tag{2.5}$$

provided that the thermal conductivity c is independent of temperature. Here T_0 is the initial density and ρ is the density of the conductor.

Special attention should be paid to the fact that $\bar{h}$ is a function of the initial temperature. In Table 1 all data are listed for the room temperature. In Ref. [14] the quantity $\bar{h}$ was shown to increase 2 to 2.5 times on decrease of T_0 to 4 K for metals such as W, Mo, Nb. Conversely, the greater the temperature T_0, the lesser is the specific action $\bar{h}$.

2.2 Microexplosions at the cathode and the ecton model

Let a microexplosion be excited at the tip of a conical cathode through Joule heating by the current $i(t)$ in some way. In the spherical system of coordinates, the thermal balance equation at the cathode can be written in the form

$$\rho c \frac{dT}{dt} = \lambda\left(\frac{2}{r}\frac{dT}{dr} + \frac{d^2T}{dr^2}\right) + \frac{i^2(t)\,\kappa(T)}{\Omega^2 r^2} , \tag{2.6}$$

where $\Omega = 4\pi \sin^2(\theta/4)$ is the solid angle; θ is the cone angle; r is the radius in the spherical system of coordinates; λ is the thermal conductivity. The other parameters were mentioned earlier.

For a plane cathode $\theta = \pi$, and therefore $\Omega = 2\pi$. In the study of ectons, of concern will be small times $t \leqslant 10^{-8}$ s. Therefore, the heat conduction can be neglected at the

initial stage. Given that ρ and c are independent of temperature and $\kappa = \kappa_0 T$, we have

$$T = T_0 \exp\left[\kappa_0 \int_0^{t_d} i^2(t)\,dt \left(16\pi^2 \rho c r^4 \sin^4\frac{\theta}{4}\right)^{-1}\right]. \quad (2.7)$$

The radius r_{ex} may be found from Eqn (2.7). For it the temperature is greater than the formal critical one in the explosion:

$$r_{ex} = \left[\kappa_0 \int_0^{t_d} i^2\,dt \left(16\pi^2 \rho c \sin^4\frac{\theta}{4} \ln\frac{T_{ex}}{T_0}\right)^{-1}\right]^{1/4}. \quad (2.8)$$

All the metal inside this radius is presumed to have exploded.

In our pursuit to construct the simplest ecton model, the first supposition will be that Eqn (2.5) may be employed in formula (2.8), and the experimentally measured quantity $\bar{h}$ may be used as the specific action. In this case, formula (2.8) can be written in the form [1]:

$$r_{ex} = \left[\int_0^{t_3} i^2\,dt \left(16\pi^2 \bar{h} \sin^4\frac{\theta}{4}\right)^{-1}\right]^{1/4}. \quad (2.9)$$

As was mentioned above, the ecton functions for a limited time since the explosive centre rapidly cools down owing to heat conduction, ejection of heated atoms and ions of metal, and a decrease in the current density because of increase in the radius of emission.

The second supposition will be that the ecton cools down owing to the heat conduction and an increase in the radius of the explosion zone. The ecton stops functioning once r_{ex} is equal to the heat path length r_λ because of heat conduction. In this case

$$r_{ex} = r_\lambda = 2(at)^{1/2}, \quad (2.10)$$

where $a = \lambda/\rho c$ is the thermal diffusivity, and t is time. Let r_e be the radius for which this condition is satisfied. Then it follows from Eqns (2.9) and (2.10) for $i = \text{const}$ that

$$r_e = i\left[8\pi(a\bar{h})^{1/2} \sin^2\frac{\theta}{4}\right]^{-1}, \quad (2.11)$$

and the time for which the ecton functions is

$$t_e = i^2\left(256\pi^2 a^2 \bar{h} \sin^4\frac{\theta}{4}\right)^{-1}. \quad (2.12)$$

The mass of metal carried away in a microexplosion is $m_e = (4\pi/3) r_e^3 \rho \sin^2(\theta/4)$. If r_e is the same as in Eqn (2.11) we have

$$m_e = \rho i^3 \left[384\pi^2 (a\bar{h})^{3/2} \sin^4\frac{\theta}{4}\right]^{-1}. \quad (2.13)$$

The overall charge of electrons carried away by the ecton is $q_e = i t_e$. With consideration for Eqn (2.12), this matches the number of electrons in the ecton

$$n_e = i^3\left(256\pi^2 a^2 e\bar{h} \sin^4\frac{\theta}{4}\right)^{-1}, \quad (2.14)$$

where e is the charge of an electron. The mass carried away from the cathode per unit charge is $\gamma_m = m_e/q_e$, or

$$\gamma_m = \frac{2}{3}\rho\left(\frac{a}{\bar{h}}\right)^{1/2}. \quad (2.15)$$

Consequently, in this model the specific mass carried away depends solely on the properties of the material out of which the cathode is made. In Table 2 [15] the thermal diffusivity a and density ρ required in subsequent estimations are listed for various metals.

Table 2.

Metal	Cu	Ag	Au	Al	Mo	W	Fe	Ni
a/cm^2 s^{-1}		1.6	1.2	1.4	1.0	1.5	1.6	1.5
ρ/g cm^3		8.9	10.5	19.3	2.7	10.2	19.3	

Now I want to dwell briefly on the current density while an ecton functions. In field emission initiation, the initial current density is determined from the relationship for the specific action:

$$j = \left(\frac{\bar{h}}{t_d}\right)^{1/2},$$

where t_d is the explosion delay time. Since $\bar{h} \sim 10^9$ A^2 s cm^{-4}, the current density is about 10^9 A cm^{-2} for $t_d \sim 10^{-9}$ s. The current density is

$$j_e \approx 16\pi a \bar{h} i^{-1} \sin^2\frac{\theta}{4} \quad (2.16)$$

at the final stage of the functioning of an ecton.

After the explosion the plasma starts to scatter. In Ref. [4] the author proposed an adiabatic model for the scattering of plasma. Let a specific energy w_0 be delivered to a volume of the cathode. In the course of scattering, the energy is transformed into the kinetic energy of the particles of plasma. If the plasma radius becomes much greater than the characteristic size of the initial volume, it follows from the law of conservation of total energy in a volume of particles that the velocity v_p of the forward layers of plasma is related to the specific energy w_0 by the equation:

$$v_p \approx \left(\frac{4\gamma}{\gamma - 1} w_0\right)^{1/2}, \quad (2.17)$$

where γ is the adiabatic exponent. The adiabatic exponent is $\gamma = 1.24$ for the scattered plasma [16].

The velocity of scattering of plasma is $(1-2)\times 10^6$ cm s^{-1} for metals such as W, Mo, Cu, Al, Ni, Pl, and others. Therefore the specific energy is $w_0 = (2-8)\times 10^4$ J g^{-1} before the explosion. In plasma produced in microexplosions, there are singly, doubly, and even triply charged ions. These ions have very high energies. For example, singly charged ions of copper of the velocity 1.5×10^6 cm s^{-1} are accelerated to 70 eV.

Let us consider now the cause of the cut-off of current in the ecton. This issue is tightly linked to the mechanism of electron emission from a metal. To all appearances, this is the thermionic emission enhanced by the Schottky effect at the expense of the electric field at the plasma–metal interface. Within the framework of the classical thermal model, the growth of the temperature is assumed to be much higher than the boiling temperature within the time 10^{-9} s. Assuming that the Richardson–Schottky formula is true under the cited conditions,

$$j = AT^2 \exp\left(-\frac{e\varphi - \alpha E^{1/2}}{kT}\right), \quad (2.18)$$

where $A = 120.4$, $\alpha = 3.79 \times 10^{-4}$; φ is the work function ($\varphi = 4.4$ eV for copper); k is Boltzmann's constant; E is the electric field on the emitting surface, V cm^{-1}; T is the temperature at the cathode, (K); j is the electron current density, A cm^{-2}. Simulation of processes in an ecton

showed that the field E is not larger than 10^5 V cm^{-1}. According to estimations for copper the current density is 10^8 A cm^{-2} when the energy delivered is equivalent to 10^4 K and is only 5×10^6 A cm^{-2} when 7×10^3 K, i.e. the cooling of the ecton by 30% results in the decrease in the current density by a factor of 20.

Thus the qualitative pattern of the break of current in an ecton is as follows. Initially the current density in the ecton is about 10^9 A cm^{-2}. Then the microvolume is rapidly heated and exploded. The explosion results in efficient thermionic emission. As the explosion proceeds, the emission zone expands and the heat dissipates and is carried away through evaporation and ejection of heated liquid metal. All the above processes are responsible for decreases in the temperature of the zone in which the ecton functions and in the thermionic emission current density. In its turn, the decrease in the emission current density causes the emission zone to cool down more rapidly, as the Joule heating decreases.

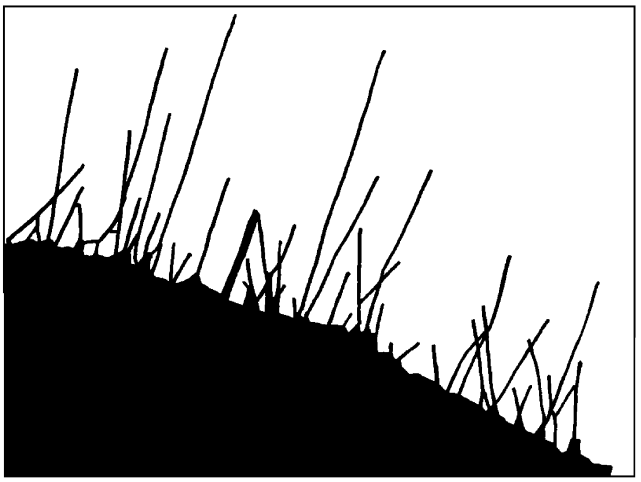

Figure 2. Filamentary crystals at a cathode of gold.

3. Surface of electrodes

3.1 Microgeometry of electrodes.

It is impossible to produce a cathode with an absolutely smooth and pure surface. For the excitation of an ecton, three types of imperfections are responsible: micropeaks on the surface; gas adsorbed at the surface; and also dielectric films and embedments. Let us consider them in more detail. The surface of a cathode has microirregularities due to various causes. For example, when machined, the grains of the crystal structure are destroyed and an amorphous layer is formed. Usually such an electrode is put through electric polishing. Then the upper layer is removed and the crystalline structure of the metal is revealed. As a result of such a procedure, the projecting parts are substantially dissolved. However, electric polishing does not ensure that peaks the radius of the tip of which is a fraction of a micron will be totally removed. Their presence was verified by direct observations with an electronic microscope [17].

The microrelief of the metallic surface is changed significantly under heating. The surface energy of metal decreases since faces of crystals with lesser surface tension appear. The appearance of microirregularities at electrodes is favoured by evaporation and condensation, recrystallisation, phase changes, etc., which manifest themselves even before the metal is heated to the melting temperature. The fast cooling of metallic specimens heated previously produces peaks on the surface which are similar to compound spicular patterns [19]. Under prolonged tension, the surface microrelief is distorted significantly. Processes such as surface diffusion, rearrangement in electric field, evaporation, desorption by the field, migration of impurities, etc., can proceed [20–22]. The irregularities on the metallic surface are especially large when there are filamentary crystals [23, 24]. In such crystals, the ratio of the height to the radius can exceed 1000. They are formed when supersaturated vapours are condensed at electrodes (Fig. 2). The microrelief of a cathode in vacuum is significantly changed in electric discharges. The discharge current causes the electrode to erode owing to thermal processes. The erosion is accompanied by the formation of craters, micropeaks, and ejection of microdroplets of metal onto the surface.

The notion of the electric field gain β_E is introduced to provide a quantitative characteristic for the surface of a cathode. This is the ratio of the true value of the electric field at the top of a micropeak to its mean microscopic value. Given $\beta_E \gg 1$, the approximate relationship $\beta_E \approx h/r$ can be used [22, 25].

The quantity β_E may be determined by measuring the autoelectronic current in vacuum as a function of the electric field strength. The current from the point is described by the Fowler–Nordheim equation:

$$i = A \frac{\beta_E^2 E^2 S_{\text{em}}}{\varphi} \exp\left(-B \frac{\varphi^{3/2}}{\beta_E E}\right), \qquad (3.1)$$

where E is the electric field at the tip of the peak; S_{em} is the emission area; φ is the work function; A and B are quantities from the Fowler–Nordheim formula. It follows from Eqn (3.1) that the curve $\log(i/E^2) = f(1/E)$ is a straight line. In this case given the work function φ, the electric field gain β_E may be evaluated from the slope of the straight line, and the emission area S_{em} from the length of the gap the straight line intercepts the abscissa axis.

Of special interest are studies which enable the parameters of peaks to be evaluated directly. In Refs [17, 18] the emission centres were sought with the aid of a luminescent anode which glowed at the points where electrons were incident. In the overwhelming majority of cases, micropeaks were detected at centres of emission. Then the profiles of these micropeaks were viewed through a shadow electron microscope. The electric field increases by a factor of 100 or more according to the authors of Refs [17, 18]. Similar peaks were detected on electrodes made of copper, nickel, tungsten, aluminium, tantalum, and stainless steel.

In Refs [26–28] emission centres were detected by the method of probing anode opening and then were examined with an x-ray microanalyser; and the energy spectrum of emitted electrodes was also recorded [26]. The spectrum of centres detected on the faces of the grains of the crystal lattice was the same as that of electrons, with the peak shifted to low energies which are typical of semiconductor emitters. The x-ray analysis showed a submicroscopic region on the face of a grain. The region contained lines of impurities Al and Fe entering into the composition of the metal, the oxides of which are used to produce the electrodes. Upon an electron bombardment the lines of

impurities disappeared and the emission centre disappeared with them. The cited analysis shows that β_E can vary over a wide range (from 10 to 1000). However, many researchers believe values of the order of 1000 to be too large, though points with such β_E were observed experimentally. Therefore, additional research should be performed to explain this contradiction. Erroneous evaluations could be made at least for the following reasons.

First, the dimensional effect: at room temperature the free path length of an electron is about 5×10^{-6} cm in metal and it drops inversely proportionally to temperature. Hence, the dimensional effects can influence the processes of release and dispersion of energy in an emitter. Second, probably the Fowler–Nordheim equation, as applied to very sharp micropoints, should itself be refined fundamentally. It was deduced for an infinite plane that micropoints are very inhomogeneous configurations the radii of which are of order of tens to hundreds of the atomic radius. Third, the value of the parameter β_E depends on the gas adsorbed at the cathode [4, 17] and also on the dielectric film.

3.2 Gas adsorbed at electrodes

The surface adsorption is the adsorption of gas or vapours of a fluid onto the surface of a solid body [24]. Chemically the adsorbent has atoms with unsaturated valency on its surface. This means that on the surface of a solid body there are parts which provide for chemical bonds with adsorbed particles. The surface energy lowers as a result of adsorption. The concentration of free chemical bonds decreases as the number of adsorbed particles increases. Particles in number sufficient to saturate all surface bonds form a monolayer. This typically occurs when there is one adsorbed atom for four surface atoms [30], which corresponds to the density of adsorbed atoms of 10^{14} cm^{-2}.

For bonds of adsorbed particles in a monolayer, the chemical forces are responsible. Therefore an adsorption of this type is called chemical adsorption or chemisorption. Here an adsorbed molecule gives away an electron to or receives it from the surface. It may be split into atoms or radicals which form bonds with the surface. This is typical of molecules of oxygen, nitrogen, hydrogen, and others. New bonds between radicals are possible in the adsorbed layer. In chemical adsorption, the bond energy is high enough and amounts to several electron volts per particle.

Adsorption should be considered as a dynamic process in which at equilibrium the number of atoms leaving the surface in a unit time owing to thermal motion is equal to the number of newly adsorbed atoms. At equilibrium, $nv/4$ molecules drop in a unit time onto the surface bordering the gas. Here n is the gas density and v is the mean velocity of molecules. At room temperature and the pressure of 1 mm Hg, $n \approx 3.7 \times 10^{16}$ cm^{-3} and $v \approx 4.5 \times 10^4$ cm s^{-1}. Given the probability of adhesion to the surface to be equal to 0.5, the rate of adsorption is 2.5×10^{20} particles cm^{-2} s^{-1}. Thus, the monoatomic layer forms approximately in 10^6 s at the pressure 1 mm Hg. Hence, in a gas a surface is always coated with at least one film of atoms or molecules.

A solid body at the surface of which there is a monolayer of adsorbed atoms has no free valences. Therefore the formation of new layers is caused solely by the van der Waals polarisation forces. This is a physical adsorption since there is no exchange of valence electrons between atoms of gas and metal. In physical adsorption, the bond energy is well below that in chemical adsorption, and it is of the order of fractions of an electron volt per atom. One and the same gas adsorbs onto different metals differently. In this respect oxygen is the most active gas. It adsorbs virtually onto all metals.

The work function of electrons is different when atoms are adsorbed onto a metallic surface. When adsorbing, electronegative atoms capture a free electron. As a result, the intensity of the double electric layer near the metal increases, which hinders the escape of an electron and results in growth of the work function. Conversely, the presence of electropositive atoms on the surface results in a drop in the work function for the cathode material.

3.3 Dielectric films and embedments on surfaces of metals

In atmospheres capable of oxidising electrodes, the cathode is coated in a layer of oxides. In addition, impurities and dielectric embedments could be left after the polishing at the cathode, and so too could dielectric embedments of the material itself which appear upon the removal of the surface layer by electrochemical polishing or ionic etching [27].

Clearly, it is difficult to control such impurities at the cathode in the gas discharge directly. Therefore the special term 'uncontrolled dielectric embedments at the cathode' is sometimes used in the literature. However, these embedments are of importance for many types of discharge. It is common knowledge that autoemission currents build up when ions are deposited onto a dielectric film (the Malter effect).

The dielectric film can be broken down when electric fields which the electric charges of ions are responsible for are high enough. If there is a dielectric film at the cathode, then its outer surface is charged by the flow of positive ions to the cathode when the specific resistance of the film is large. Once the field reaches the breakdown value, the film is broken down and the cathode is eroded locally at the site of breakdown.

Most of the results from which numeric dependences can be reproduced were obtained for specially prepared dielectric films. A metallic layer is first deposited onto a base and then it is overlayed by any method (thermal cooling, chemical precipitation from gas phase, diffusion) with a layer of dielectric: Al_2O_3, SiO_2, Si_3O_4, etc. The upper electrode is often coated too. The structure of the metal–dielectric–metal type (MDM) is often used in thin-film capacitors, in nonincandescent cathodes, and in microelectronic devices.

In the production of MDM structures, all procedures are aimed at obtaining a dielectric film of electric strength as large as possible. Therefore, special attention is paid to spray coating in which the geometric inhomogeneity of the base is minimal and the dielectric material has no through and closed pores. However, this pattern is an ideal one.

The density of pores per unit area is 0.3–0.4 mm^{-2} for films SiO_2 and SiO_4, prepared by thermal oxidation, the typical thickness of which is 0.5 μm. Because of this, the breakdown intensities of thin films vary widely. The breakdown intensity is $E_b = U_b/d$, where d is the film width; E_b is a mean value characterising the state of electrodes as well as ionisation.

The actual breakdown intensities $E_b > 10^6$ V cm^{-1} suggest that electron field emission inward from micro-

peaks at the cathode contributes to the mechanism of breakdown. In several models [34], the breakdown is assumed to have occurred once a critical current density of field emission is reached. This current heats up micropeaks and adjacent areas. As a result of evaporation of metal and dielectric and also because of ionisation, the current builds up and the electrodes are eroded. In essence, the process in question is the excitation of an ecton on the surface of metal.

4. Excitation of ectons

4.1 Explosions of micropeaks

According to results on explosions of cylindrical conductors, the explosion delay time is 10^{-9} s for the current density 10^9 A cm^{-2}. There are many ways in which such high current densities can be reached. The simplest one is the field emission (FE) from points of small radii (micropeaks). It has long been believed that FE and its different modifications is the only factor responsible for an EEE. However, this is not necessarily so. The concentration of energy in microvolumes of conducting media and excitation of ectons can owe their origin to the presence of a dielectric medium in the cathode area; interaction of plasma with the cathode, and plasma with dielectric and metal simultaneously; gas desorption from cathode; laser radiation to cathode; and impact of an accelerated microparticle on the cathode, etc.

The FE current density may be found from the Fowler–Nordheim formula (FN):

$$j = 1.55 \times 10^{-6} \frac{E^2}{t^2(y)\varphi^2} \exp\left[-6.85 \times 10^7 \frac{\varphi^{3/2}}{E}\theta(y)\right], \quad (4.1)$$

where φ is the work function in electron volts; j is the current density in amperes per square centimetre; E is the electric field strength in volts per centimetre; $t(y)$ and $\theta(y)$ are functions of

$$y = 3.62 \times 10^{-4} E^{1/2}\varphi^{-1} . \quad (4.2)$$

In practical calculations it can be assumed that $t(y) \approx 1$, $\theta(y) = 0.95 - 1.03y^2$.

It follows formally from Eqn (4.1) that the electron current of density up to 10^{10} A cm^{-2} or more is possible. However, the dependence $j(E)$ diverges from the Fowler–Nordheim law even for the current density about 10^8 A cm^{-2}. This manifests itself in a slower growth of emission current (Fig. 3) [41]. It turned out that this effect was typical of all metals studied (W, Mo, Ta, Re, etc.). The higher the current density and the lower the work function, the higher is the deviation. This effect is due to two reasons: the influence of the space charge of emitted electrons and the progressive contribution of the potential in the region near the surface as the electric field grows owing to quantum-mechanical effects. The influence of the space charge on the trend of $j(E)$ is predominant when the electric field and current density are large.

When the influence of the space charge is essential, the dependence $j(E)$ is described by the Child–Langmuir law which has the form [35, 36]:

$$j = \frac{4}{9}\varepsilon_0 \left(\frac{2e}{m}\right)^{1/2} E^{3/2} v_{em} r_{em}^{-1/2} , \quad (4.3)$$

where the coefficient v_{em} is a function of the shape and size of the emitter and is of the order of unity; r_{em} is the radius

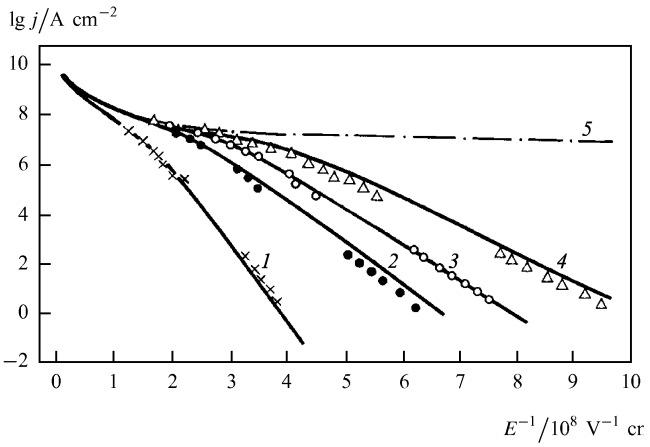

Figure 3. The comparison between the experimental data and the FE theory with consideration for space charge. Given for various values of the work function φ (eV) of metal: (*1*) 4.50; (*2*) 3.19; (*3*) 2.80; (*4*) 2.44; (*5*) the Child–Langmuir curve.

of the emitting area; ε_0 is the dielectric constant. Curve *5* in Fig. 3 is the dependence [Eqn (4.3)]. In many studies it was shown that the current density up to 10^9 A cm^{-2} can be reached in a tungsten emitter under pulse voltage when the pulse duration is $10^{-9}-10^{-6}$ s [35, 37]. Microemitters explode when the current density becomes large.

The limiting FE current density depends also on the geometry of the emitting point. The limiting current density is 0.4×10^8, 0.6×10^8, 0.7×10^8, and 1.0×10^8 A cm^{-2} for the opening of a cone 3°, 5°, 6°, and 16°, respectively, when tungsten points are cones, the pulse duration is 1 μs, and the radius of the emitter is 0.15–0.3 μm. A larger current density for larger angles can be explained by better conditions for withdrawing the heat from the top of the emitter. As is shown in Section 3, there are micropeaks on any surface which is believed to be smooth. Therefore, ectons are excited not only by explosions of specially prepared micropoints, but also by explosions of microparts on a flat surface owing to the FE current.

If a cathode is a liquid metal, then the surface structure is changed under the action of electrostatic forces. Tonks considered the balance of forces of surface tension, gravity, and electrostatics [38]. The instability condition for a horizontal plane of liquid metal has the form:

$$\varepsilon_0 \frac{E^2}{2} > \frac{\alpha}{r} + \rho g r , \quad (4.4)$$

where ρ is the density of material; α is the surface tension coefficient; g is the acceleration of the force of gravity; r is the radius of the liquid surface. The smallest value of the field E under which the fluid surface is disturbed corresponds to the optimal value $r = r_0$ for which both sides in Eqn (4.4) are equal. For example, the field strength for which the surface is disturbed is $E = 53$ kV cm^{-1} for mercury, and $r_0 = 0.37$ cm [39].

Once inequality (4.4) holds on the surface of liquid metal, a hunch appears and begins to grow. The electric field strength increases on its surface, which results in extension of fluid at this site. Initially the hunch is shaped almost like a ball segment (Fig. 4) but is then transformed into a tapering cone, where the height

$$h \approx \frac{\alpha}{\varepsilon_0 E^2} . \quad (4.5)$$

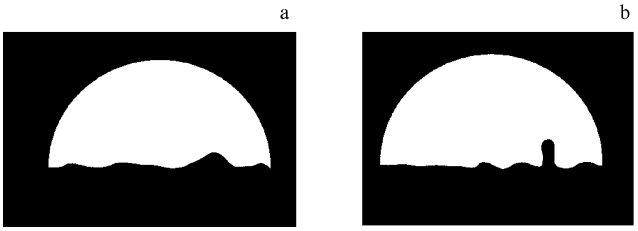

Figure 4. The growth of a micropeak at the surface of mercury for different electric fields between electrodes. The field in case (a) is less than that in case (b) [39].

Note that the radius of the tip does not decrease. Such a peak can explode under the action of FE current or it can break off and fly to the opposite electrode.

The capability of a liquid metal to concentrate energy in a microvolume at the cathode, in the presence of an electric field, suggests another view of the melting of metal at the cathode. The metal can be melted by beams of ions, plasma, laser radiation, etc. Experiments testify that micropeaks can form as a result of melting of metal in an electric field [40]. A copper flat plate was exposed to plasma radiation in the presence of an electric field 100 kV cm^{-1}. On an abrupt reduction of bombardment, the surface solidified fast so that an uneven microrelief remained. As will be shown later, such a peak, when placed in plasma, can bring about an increase in the current density at the site of contact of the peak and another metal. This favours the explosion of the peak.

Numerous experimental data cited in [4] show that the following two criteria are true for explosions of points:

$$j = \text{const}_1 \tag{4.6}$$

in a steady regime, and

$$\int_0^{t_d} j^2 \, dt = \text{const}_2 \tag{4.7}$$

in an unsteady regime. Here j is the current density at the contact of the point, t_d is the explosion duration, and the constants characterise the material out of which the cathode is made and the shape of the micropoint.

One of the principal issues in the theoretical description of initiation of an ecton by the FE current is to explain the dependences given by Eqns (4.6) and (4.7). It turns out that the simplest explanation may be given within the framework of the Joule model for the heating of a point. The limiting current density

$$j = \frac{1}{h}\left(\frac{\lambda}{\kappa_0}\right)^{1/2}, \tag{4.8}$$

when a cylindrical point cathode is heated by the FE current in a steady state. Here h is the height of the peak and λ is thermal conductivity. For example, $j = 2 \times 10^8$, 0.5×10^8, and 0.25×10^8 A cm^{-2} for copper, tungsten, and nickel when the height h of the peak is 1 μm.

For short pulses the limiting FE current density exceeds that in steady state. If the pulse duration is much less than the time for which the system goes into steady state, then the inequality

$$t_p \ll \frac{h^2 \rho c}{\lambda} \tag{4.9}$$

is true. Here t_p is the pulse duration. For example, if $h = 0.6\,\mu m$ for tungsten, then Eqn (4.9) holds even for $t_p = 10$ ns.

If inequality (4.9) holds and the initial current density j does not change in time, then the temperature of a cylindrical emitter grows exponentially in time in accordance with the law

$$T = T_0 \exp \frac{j^2 \kappa_0 t}{\rho c}. \tag{4.10}$$

If the point is conditionally assumed to explode when a critical temperature T_{ex} is reached, then the explosion delay time may be determined from Eqn (2.6), which is analogous to Eqn (4.7).

Thus, the simple Joule model of heating of a point explains the basic experimental criteria, given by Eqns (4.6) and (4.7), correctly. However, many researchers found that the 'Nottingham' effect plays an important part in the energy balance at the tip of an emitter [41]. When the electric field strength at the cathode is large, the potential barrier at the metal–vacuum interface is narrow and the probability of electron tunneling through the barrier is nonzero. Since conduction electrons in the cathode metal exist predominantly at energy levels that are below the Fermi level for low temperatures, the emission into vacuum occurs predominantly from them. Hot electrons are accumulated near the emitting surface. Therefore the electron gas temperature grows, i.e. the Nottingham effect is a heating one. As the temperature of the emitter grows, a progressively larger number of electrons acquire energies exceeding the Fermi energy and its release ceases. The temperature for which the release ceases is called the inversion temperature and is denoted by T_i. At this point, this effect becomes a cooling one.

It is interesting that equalities (4.6) and (4.7) are qualitatively the same even though the Nottingham effect comes into play. Only the constants are somewhat changed. Therefore, I shall not consider the theory of initiation of ectons by the FE current taking account of this effect. The relevant information may be found in Refs [35, 42].

4.2 The role of dielectrics

As is shown in Section 3.3, there are dielectric films on the metallic surface. Films of thickness 100 Å significantly affect the electron tunneling from metals. In these conditions the scattering of electrons within the film can be neglected. However, the theoretical consideration of the problem is made difficult by the fact that the energy distribution of surface states is unknown at the metal–dielectric–vacuum interface.

The formula

$$j = \frac{2he^3E^2}{\pi^3 ma^2Q^2} \exp\left(-\frac{v^2Q^2}{4E}\right). \tag{4.11}$$

was proposed in Ref. [41] for the emission current density under the assumption that the dielectric is homogeneous and ideal. Surface states and contact potential difference were not considered. Here h is the Planck constant; e is the charge of an electron; a is the dielectric lattice constant; Q is the width of the energy gap of the dielectric; m is the mass of an electron, and $v = (\pi/h)(e/ma)^{1/2}$.

It was assumed in deriving formula (4.11) that the field is homogeneous within the film and all the electrons emitted by the metal pass into vacuum unimpeded. In terms of the

F–N variables, the plot of Eqn (4.11) is a straight line. Evaluations shows that β_E can amount to several tens of units. Latham states in Ref. [43] that in these conditions a high-density FE may be obtained when there are no peaks at the cathode. He showed that the energy spectrum of emitted electrons is displaced from the base Fermi level of the principal material, out of which the cathode is made, to low energies and the displacement is a function of voltage applied to the vacuum gap.

The breakdown of a thick dielectric film when it is charged by ions plays an important part in initiating an ecton. The film is broken down once the electric field becomes high enough. The breakdown current initiates an ecton. This process will be discussed in detail in Section 4.3, where the role of plasma in the initiation of ectons is discussed.

One of the most common ways of exciting an ecton is the discharge over the surface of a dielectric in vacuum when it comes in contact with metal. The metal–dielectric–vacuum contact point is called a triple point (TP). This effect is well illustrated by the example of the excitation of an ecton at the tip of a metallic needle in vacuum when the needle rests against a dielectric plate. The opposite side of the plate is metallised (Fig. 5) [44]. Here needle *1* is the cathode, plate *3* is the anode, and metallic electrode *4* sprayed upon dielectric *2* is a trigger. Let the cathode be grounded and let a voltage insufficient to excite an ecton be applied to the anode. Now if a voltage pulse is applied to the trigger electrode, then a discharge over the dielectric starts from the electrode K. Moreover, this discharge stops at the micropoint of the cathode resting against the dielectric (Fig. 5). If this current is large enough, the micropoint explodes and an ecton occurs from the metallic emitter *1* to the flat anode *3*. The discharge current over the surface of the dielectric owes its existence to the dynamic capacity. The dynamic capacitor is the gap between the plasma on the surface of the dielectric and the metallic layer on the opposite side of the dielectric.

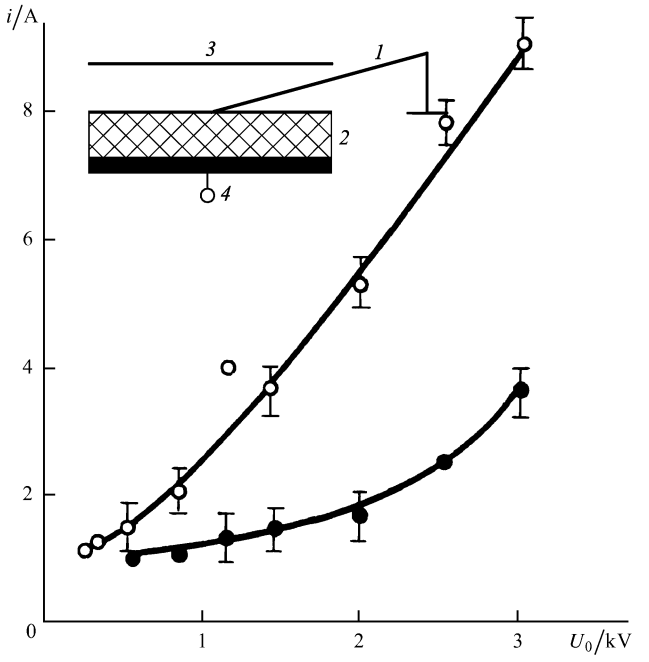

Figure 5. In the upper part, the scheme of excitation of an ecton at the triple point is shown: (*1*) cathode; (*2*) dielectric; (*3*) anode; (*4*) trigger. In the lower part, the discharge current is plotted as a function of the voltage amplitude for dielectrics of barium titanate of a width 2 mm in cases: electrode *1* is a cathode to electrode *4* (hollow circles) and electrode *1* is an anode (full circles).

This is a very efficient and simple way of exciting an ecton. It is used in developing various types of vacuum gaps and metal–dielectric cathodes with explosive electron emission. In this case a metallic net is spread over the dielectric surface [45] or metallic bars are seared [46]. Dielectrics with large dielectric permeability ε (for example, ferroelectrics) are used to increase the performance of such cathodes [45].

Let us consider in more detail when an ecton occurs at a TP [47]. The current about a TP is determined from the relationship $i = U_0\,\mathrm{d}C/\mathrm{d}t$, where C is the dynamic capacity. The plasma velocity over the surface of a dielectric is $v_D \sim AU_0^2$, where A is a function of the kind of dielectric and its thickness [44].

If $tv_D \ll \delta$, then $C = 4\varepsilon_0\varepsilon v_D t$, where ε_0 and ε are the absolute and relative dielectric permeabilities. Consequently, the current is $i = 4\varepsilon_0\varepsilon AU_0^2$. This current will flow in the metal–dielectric contact through the area $S_c = \pi r_c^2$ (Fig. 6). Therefore, the current density through this contact is $j_c = 4\varepsilon_0\varepsilon A\,U_0^2/\pi r_c^2$.

The metallic contact will explode within time $t_d = \bar{h}/j_c^2$, where $\bar{h}$ is the specific action. The time t_d is determined from the relation

$$t_d = \frac{\pi^2 \bar{h} r_c^4}{16\varepsilon_0^2\varepsilon^2 A^2 U_0^4}\,. \tag{4.12}$$

An ecton occurs at the TP when the time t_d is less than the start pulse duration t_p, that is, when $t_d < t_p$. Then the inequality

$$r_c < \left(\frac{16\varepsilon_0^2\varepsilon^2 A^2 t_p U_0^4}{\pi^2 \bar{h}}\right)^{1/4} \tag{4.13}$$

follows from Eqn (4.12) for the radius r_c. For silver contact $\bar{h} = 0.8 \times 10^9$ A^2 s cm^{-4}. If $t_p = 10^{-7}$ s, $\varepsilon \approx 10^3$, $U_0 = 10^3$ V, $A = 5 \times 10^2$ cm s^{-1} V^{-1}, then it follows from Eqn (4.13) that $r_c < 2 \times 10^{-5}$ cm. It follows that all triple points the radii of contact of which are less than 10^{-5} cm will explode, and ectons will occur when the pulse duration is $t_p = 10^{-7}$ s.

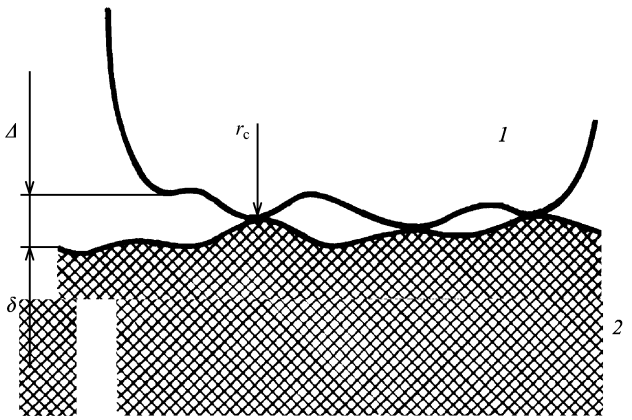

Figure 6. Scheme of the contact between metal (*1*) and dielectric (*2*).

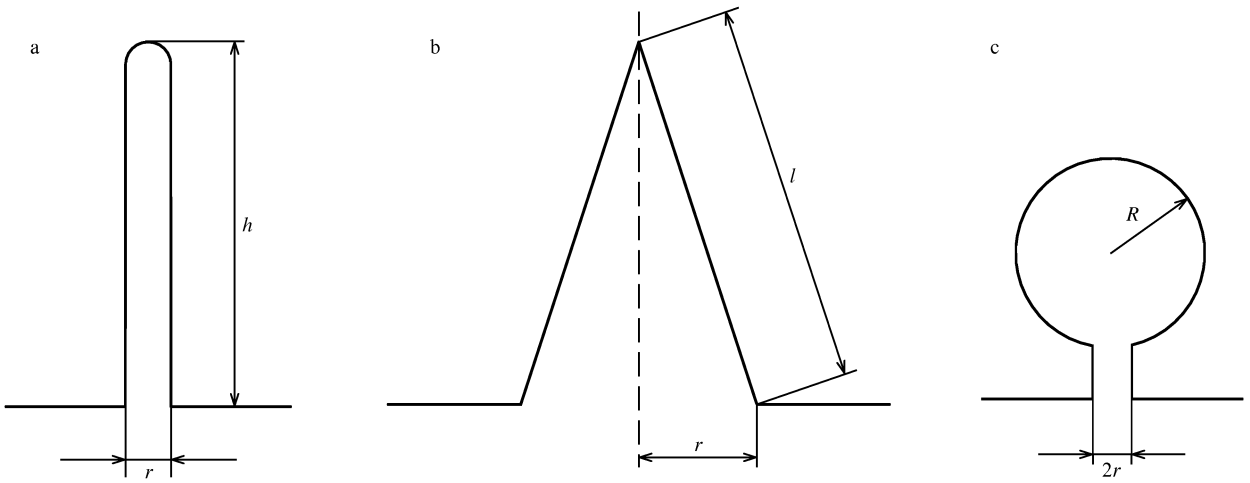

Figure 7. Configurations of inhomogeneities for determining the current density gain at the cathode: (a) cylinder; (b) cone; (c) sphere.

4.3 The role of plasma

It has long been known that a vacuum discharge may be excited by the action of plasma on the cathode. As is shown in Ref. [4], ectons occur at the vacuum discharge stage when the current builds up in the cathode–anode gap. There are two types of ectons at the cathode: when dielectric films and embedments are present and when they are absent.

In Ref. [4] the formation of an ecton is described when the cathode is bombarded by plasma from a plasma gun. Plasma runs onto the near cathode. Ectons occurred at a cathode at which dielectric impurities were surely detected. This shows that energy is concentrated in a microvolume of the cathode. The probability of occurrence of an ecton was the largest over distances <100 μm. The nearer the source of plasma, the greater was the probability. The smallest plasma concentration was 10^{16} cm^{-3}. Ectons were not observed at thoroughly purified and degasified cathodes.

In Ref. [48] an ecton was observed at the cathode, the surface of which was thoroughly purified from oxides and impurities, when the plasma source was placed at a very small distance (5 μm) from the cathode. The plasma concentration was 10^{20} cm^{-3} and the density of current to the cathode was 10^7 A cm^{-2}. New ectons were detected over short distances (of the order of several microns) from the current oscillogram, and microcraters were seen at the cathode. How can these effects be explained?

The current density builds up at micropeaks on the cathode when plasma flows about the cathode in the presence of an electric field. Let us consider three configurations of micropeaks on a flat cathode: a cylinder, a cone, and a sphere (Fig. 7). The ion current $i_i = j_i S$ flows over the surface of the micropeak when plasma flows about such a micropeak (j_i is the ion current density and S is the area of the peak). However, when the current enters the cathode, it goes in any case through the area πr^2. Consequently, its density at the cathode is

$$j = j_i \frac{S}{\pi r^2} . \quad (4.14)$$

The area S is $2\pi rh$, πrl, and $4\pi R^2$ for a cylinder, a cone, and a sphere, respectively. The current density gain β_j is $2h/r$ for a cylinder, l/r for a cone, and $4R^2/r^2$ for a sphere (l is the cone generatrix length).

That the current density builds up is true not only of the ion current but also of any current emitted or adsorbed by the surface. For example, the surface of a micropeak ejects a thermionic emission current when the cathode is heated to a high temperature. The current density will be larger by a factor of β_j at the cathode than the average over the surface. This conclusion is also true for the inverse electron current from plasma to the cathode.

This effect plays an important part in self-maintaining microexplosive processes, i.e., in the occurrence of secondary ectons. In addition, if inhomogeneities are in the immediate vicinity of the explosive centre, then the ionic current density can be large enough for a microexplosion at the cathode to occur when the gain is taken into account. In fact, the ion current density is

$$j_i = \frac{1}{4} q_i n_i v_i , \quad (4.15)$$

where q_i is the mean charge of an ion; n_i is their concentration; v_i is the velocity of ions. Since the concentration n_i lowers away from the centre as $n_i \propto 1/x^2$, where x is the distance from the centre, it is natural to expect that the current density gain has an effect largely near the emission centre. This effect was observed in Ref. [48].

Plasma affects the concentration of energy much more if there is a dielectric film or a dielectric embedment at the cathode [49]. Let a cathode be coated in a dielectric film under which there is a metallic micropeak. If this system is placed in an electric field and plasma is conveyed to the dielectric, then the dielectric film is charged by incoming ions.

The electric field strength in the film is

$$E = \frac{j_i t}{\varepsilon \varepsilon_0} , \quad (4.16)$$

where ε is the dielectric permeability of the film and t is time. The film is broken down when the field E reaches a certain value. The breakdown current excites an ecton.

Thus, we showed that there are two ways in which ectons may be excited by plasma. One way is to charge dielectric films and embedments at the cathode by ions of plasma, and the other owes its origin to the current density gain at micropeaks on the cathode. If an ecton is initiated

when the electric field is $E > 10^6$ V cm^{-1} inside the dielectric, then it is necessary for the film to be charged and broken down in $t < 10^{-9}$ s, so that [1]

$$n_i v_i > 10^{23} \text{ cm}^{-2} \text{ s}^{-1}, \quad (4.17)$$

Here v_i is the velocity of ions and n_i is their concentration. If $v_i \sim 10^6$ cm s^{-1}, then the occurence of ectons can be expected under the action of inflowing plasma when $n_i \sim 10^{17}$ cm^{-3}.

If the current density is 10^9 A cm^{-2} in the second method mentioned above, then the inequality

$$n_i v_i > 10^{28} \beta_j^{-1} \quad (4.18)$$

must hold. Here β_j is the current density gain. Given $\beta_j \approx 10^2 - 10^3$, the concentration of plasma must be 2 to 3 orders of magnitude greater with the same velocity of ions for an ecton to be excited [1]. This explains why it is so easy to excite an ecton by plasma at an impure cathode and why an ecton is excited only for a high plasma density ($\sim 10^{20}$ cm^{-3}) at a purified cathode.

4.4 The role of adsorbed gas

Absorbed gas plays a twofold part in the excitation of an ecton. On the one hand, it affects the work function of the metal and thus contributes to the excitation of an ecton by the FE current. On the other hand, its effect on the metal is similar to that of the plasma on desorption and ionisation.

If the electric field strength is $E \geqslant 10^7$ V cm^{-1}, then field desorption occurs. If all atoms are desorbed, then the gas density near the cathode is $n_a \approx N_0/v_a t$, where N_0 is the number of adsorbed atoms per unit area, and $v_a \approx 10^5$ cm s^{-1} is the velocity of atoms in desorption. The gas layer of a thickness 10^{-4} cm with $n_a \sim 10^{18}$ cm^{-3} builds up for $N_0 \sim 10^{14}$ cm^{-2} within $t \sim 10^{-9}$ s after the voltage has been applied. This gas can initiate a breakdown when it is ionised by electrons through impact ionisation. To this end it is required that $(n_a \sigma)^{-1} \ll v_a t$ or $N_0 \sigma \gg 1$, where σ is the ionisation cross-section.

The inequality $N_0 \sigma \gg 1$ holds, for example, when there are several monolayers of adsorbed gas. However, the field at the cathode will not build up when the field current density is small since the gas is not ionised. For example, the electric field is $E \approx 6.5 \times 10^7$ V cm^{-1} for a tungsten cathode when $j = 10^6$ A cm^{-2}. This field is insufficient for the explosion of a point to occur. If there is a gas layer with $N_0 = 10^{16}$ cm^{-2} at the cathode, then the ion concentration will be 10^{20} cm^{-3} near the cathode within 10^{-9} s. It corresponds to $E \sim 10^8$ V cm^{-1}, which is sufficient for the explosion of a point within $t_d \sim 10^{-9}$ s.

Thus, the presence of an adsorbed gas at the cathode can be equivalent in effect to a double or triple electric field gain. This is the case when the outer field strength is close to a breakdown one, and the autoemission current density is large. I draw the reader's attention to the fact that the efficient gas desorption occurs even though the metal is heated to a temperature as low as several hundreds of degrees. Therefore, the production of a desorbed gas and its ionisation can result in generation of plasma at the cathode even though the thermal flux is relatively small. In its turn, the plasma stimulates the occurrence of an ecton.

4.5 Laser-excited ectons

The excitation of an ecton is often identical to the excitation of a vacuum discharge. Therefore, let us consider an experiment on the vacuum discharge excited by a laser beam directed at a cathode. Lasers operated in the modulated quality mode with the duration 10^{-8} s and less are typically used [22, 50].

The laser radiation is focused at the cathode to a spot of several millimeters in diameter. The production of plasma is observed when the specific radiation energy is $0.01 - 10$ J cm^{-2}. This energy is insufficient for the direct explosion of metal at the cathode but it is sufficient for the production of a coagulate of plasma at the cathode. Such an action leads to the heating of the surface of the cathode, desorption of gas, evaporation of metal, and also to thermionic emission.

The presence of an electric field provides for ionisation of the vapour by electrons. In addition, the gas is ionised by constant laser radiation. For example, the thermionic emission was observed from a tungsten cathode when the radiation intensity exceeded 2.5×10^7 W cm^{-2} and the laser pulse duration was 50 ns. The thermionic emission current was 0.5 A cm^{-2}. This emission was 30 s behind the laser pulse since it took time for the metal to heat up.

The mass-spectrum analysis of the ionic composition of plasma as a function of the radiation intensity showed that ions K^+, Na^+, H^+, C^+, H_2O^+, CO^+, CO_2^+, etc., were present in plasma when tungsten was exposed to the intensive laser radiation the power of which was 2×10^7 W cm^{-2}. It shows that ions of surface impurities, adsorbed gases, and vapours are predominant in the spectrum. The material out of which the cathode is made is predominant in the spectrum when the radiation power exceeds 10^9 W cm^{-2}.

In experiments on laser radiation with the wavelength 0.69 μm and pulse duration 30 ns, the minimal specific radiation energy for which a vacuum discharge occurred was 0.014 J cm^{-2} when the electric field was about 70 kV cm^{-1} in the vacuum gap, the cathode was made of the alloy, and the area exposed to radiation was 0.1 mm^2. When the specific energy increased 100 times, the vacuum discharge delay was 120 ns. The time characteristics were revealed to depend neither on the total ignition energy nor on its density at the site where it is supplied to the surface of the cathode.

Thus, these data demonstrate that the plasma the laser beam produces at the cathode initiates an ecton and causes the vacuum breakdown to occur.

In Ref. [51] ectons were excited at the cathode by a picosecond laser beam with a wavelength 266 nm. When a high-frequency voltage pulse with a frequency 3×10^9 s^{-1} was applied between the cathode and anode (3 μs), the laser radiation power density was 10^9 W cm^{-2} and it was 10^{11} W cm^{-2} for a fixed voltage.

4.6 Other methods of initiation of an ecton

Another way in which an ecton can be excited is by closing a cathode and anode in a microconductor which carries a large pulse current. The explosion of the conductor provides conditions for the excitation of an ecton at the cathode. It should be stressed that such microconductors appear naturally when contacts are broken. They are fluid metallic bridges which appear when electrodes melt as a result of the current constriction in the narrow electrode

zone [5, 52]. Therefore, in my opinion, ectons play an important part in the functioning of contacts. Similar effects take place in the electro-machining of metals and in electric-spark alloying.

Ectons also appear when a highly accelerated microscopic particle hits the cathode. In this case, an ecton can be excited in three qualitatively different ways. If the velocity of the particle is relatively moderate, then, when it hits the cathode, a microarea of the cathode heats up, gas desorbs, the cathode and the particle itself evaporate, gas and vapour are ionised, and an ecton occurs owing to the interaction between the plasma and cathode. If the particle velocity is high, it can excite a microexplosion and trigger an ecton in the direct interaction with the cathode. Finally, if the particle is a charged one, then even before the particle hits the cathode, an FE current can start to flow between the cathode and the particle, a micropart of the cathode explodes, and an ecton occurs. The interaction between accelerated microparticles and the cathode was discussed in detail in a variety of reviews and also in Ref. [22].

5. Mathematical modeling of an ecton

5.1 Erosion-emission model

The first step towards mathematical modeling of processes in an ecton is the erosion-emission model which, in essence, is the classical thermal model [53]. It allows a significant excess of temperature over the boiling temperature. This model gives a better description of processes in a crater than the simple Joule model. It takes into account the Joule heating, thermal conduction, evaporation of metal, thermionic emission with consideration of the Schottky effect owing to the electric field at the metal–plasma interface, and also the ion current to the cathode. The calculations were performed for flat and point copper cathodes and for current growth rates $di/dt \geqslant 5 \times 10^8$ A s^{-1}.

In Fig. 8 the mass M carried away from the tip of a molybdenum cathode is calculated as a function of the angle θ and the pulse duration. In the same figure, experimental curves are presented [4]. On the basis of the results given in Refs [4, 53], the following conclusions can be drawn. The cathode heats up to a temperature of about several tens of thousands of degrees for about 10^9 s. Thermionic emission occurs for such temperatures when the current density is 10^8 A cm^{-2}. As the radius of the cathode increases, the density of the current through the point drops and the temperature of the cathode lowers. Therefore, at one point, the thermionic emission stops.

In Fig. 9 the temperature distribution within the cathode is presented at different instances in time when the initial radius is $r_0 = 2$ μm, $\theta = 20°$, and $di/dt = 10^9$ A s^{-1}. It is seen from Fig. 9 that the temperature can be lower on the surface of the cathode than inside the metal.

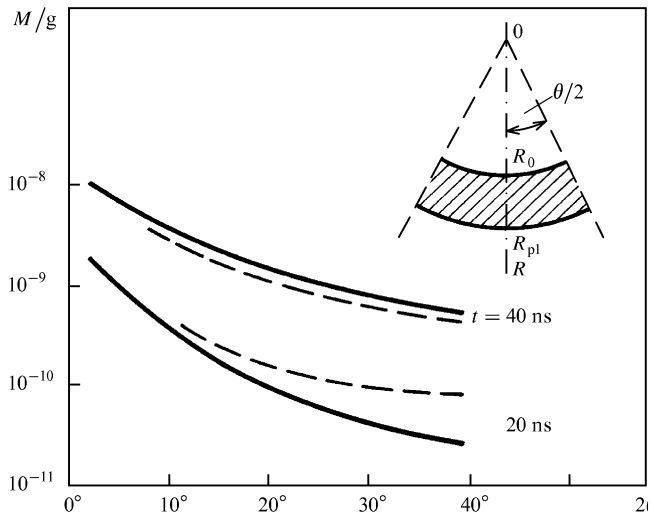

Figure 8. Mass carried away: experimental measurements (full lines) and theoretical predictions (broken lines).

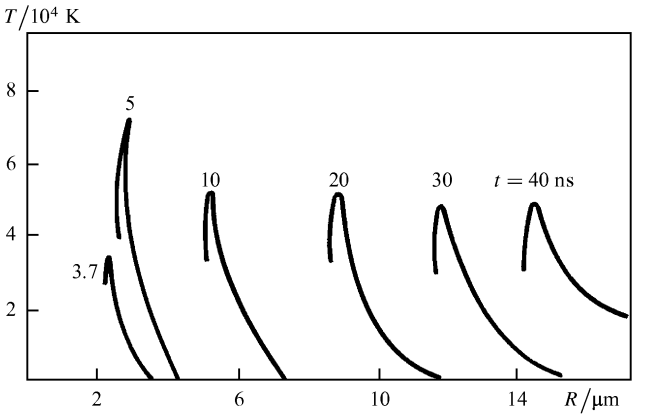

Figure 9. Temperature distribution inside a point cathode at different times.

Calculations showed that the resultant explosive emission is cyclic in nature. This is explained by the fact that, after the explosion of a microvolume in the cathode, the cathode cools down, in parallel with the Joule heating of the emission zone, owing to heat conduction, evaporation of atoms, and emission cooling. This results in drops in temperature and electric field and in the termination of emission.

Certain characteristics of an ecton at a flat copper cathode are presented at its final stage in Table 3. According to experimental data, specific erosion in the ionic phase is independent of the current, to within the error of the measurement, and is about 40 μg C^{-1} for copper [4]. Here r_{em} is the emission radius.

According to calculations, the emission zone is smaller than the melt zone. A melted depression forms mainly as a result of heat removal from hotter surface layers. The pressure of the evaporation products on the liquid metallic surface squeezes the metal to splash out of the depression. As a result, a microcrater is formed. The velocity of displacement, evaluated by the pressure, is about

Table 3.

i/A	t_{em}/ns	r_{em}/μm	$T/10^3$ K	$j/10^9$ A cm^{-2}	γ_m/μg C^{-1}
20	1	0.33	10.0	3.0	34
50	4	0.8	8.0	1.2	38
100	12	1.5	7.8	0.7	45

10^4 cm s^{-1}. The same value was obtained from the experimental data on the velocity of droplets escaping from the cathode during the discharge.

5.2 Magnetohydrodynamic calculation of the explosion of a point

The next step in the mathematical modeling was the one-fluid MHD model. As a result of the explosion, energy of large density is released in a microvolume of the cathode. The erosion products go through several phase states: the substance with density similar to the density of a solid body and with specific energy exceeding the bond energy; the mixture of gas and fluid phases; and, finally, the state corresponding to nonideal plasma with the concentration of particles $10^{20}-10^{22}$ cm^{-3} and less. Therefore, a method is necessary for the calculation of the explosion of points such that it describes all these stages subsequently.

In Ref. [54] the author used the MHD approach which was earlier developed in Ref. [10] for studying electric explosions of conductors. In this approach, the mass of the metal carried away, the temperature and velocity of plasma scattering, and its pressure at the cathode were correctly evaluated. It gave an estimate of the plasma concentration distribution, etc.

The fundamental tenets of the computational techniques are as follows [10].

(1) Processes in a material during the electric explosion of a conductor (EEC) are described by the system of one-dimensional MHD equations.

(2) The equation of state takes account of evaporation, the mixture of vapour and liquid, and also nonideal plasma.

(3) The specific resistance is a function of density and specific thermal energy. This function was found in the region of nonideal plasma by calculations and experiments ($n > 10^{21}$ cm^{-3}). The specific resistance was determined from tables for classical and weakly nonideal plasma. The tables were composed by means of numerical solutions to the Boltzmann equations and Saha relations.

Calculations were performed for copper points with a radius $r_0 = 2 \times 10^{-5}$ cm. The cone angle varied in the range $12-40°$. At $t = 0$ the density of material corresponded to that of a solid body, and the internal energy corresponded to the room temperature. The time dependence for the EEE current was taken in the form $i = a + bt$. The parameter a was chosen to be such that the current density at the point was 10^9 A cm^{-2} at the initial instant. The parameter b was, respectively, 10^9 and 10^{10} A s^{-1}.

Calculations for $b = 10^{10}$ A s^{-1} and the angle in the range from 12 to 40° showed that the point exploded by the time $t = 0.5$ s, irrespective of the angle. The specific internal energy was not uniformly distributed across the exploded material and amounted to $20-50$ J g^{-1}.

In Fig. 10a the specific energy and material density are plotted against the axial coordinate z for $r = 0$ and against the radius in a fixed layer at $t_1 = 1$ s and $t_2 = 2$ s. The plots are drawn for $\theta = 12°$. It is seen from Fig. 10 that the material is intensively heated up in a narrow layer adjacent to the unexploded metal.

The high release of energy is associated with the abrupt jump of the specific resistance of material in metal–plasma transitions. This may be seen from Fig. 10b, where the specific thermal energy w, density ρ, and specific resistance κ are presented as functions of time in one of the computational cells at the point.

The specific resistance increases drastically as w increases to 20 J g^{-1}. Then its growth rate decelerates and the energy release lowers since the current density drops when the plasma scatters. In calculations of plasma heating, the concentration was bounded from below by the value $n \approx 10^{19}$ cm^{-3}. The plasma is a two temperature one for $n < 10^{19}$ cm^{-3}, which was not taken into account.

The temperature and ionisation rate were found for $n \leqslant 10^{21}$ cm^{-3} by evaluating specific thermal energies and densities from tables of thermodynamic functions of plasma [10]. Their values fall in the ranges: $T = 3-5$ eV and $n_e/n_i = 1-3$. In calculations, the velocity of plasma scatter-

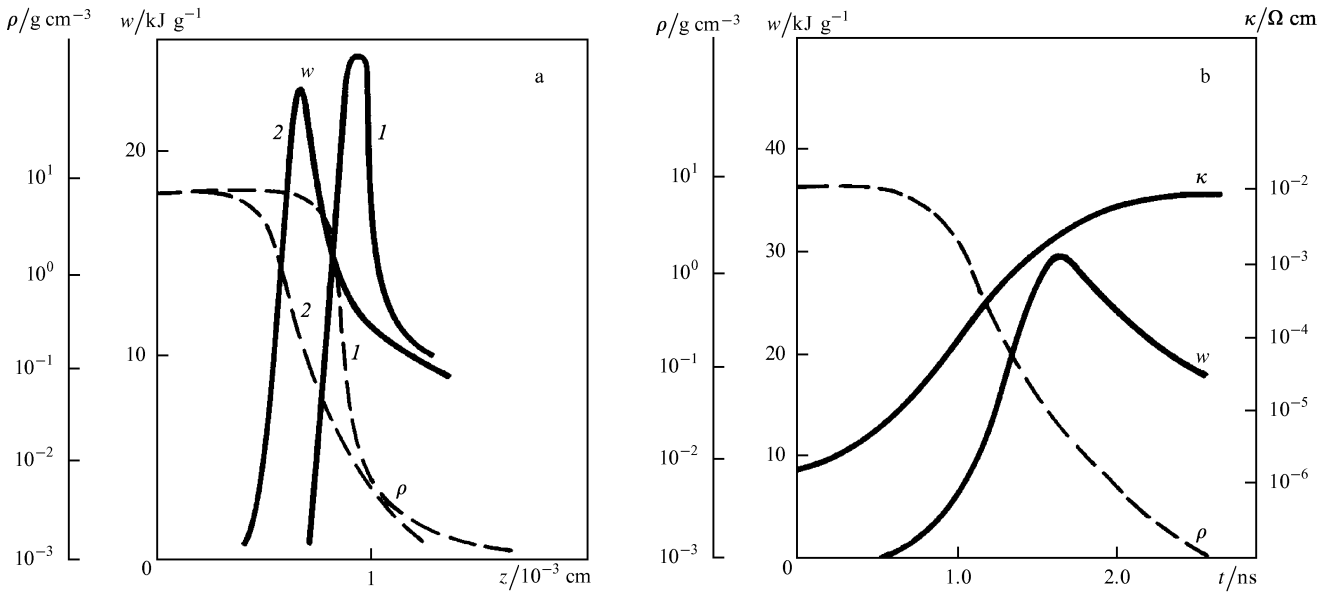

Figure 10. (a) Density and specific thermal energy distributions, ρ and w, along the point axis at $r = 0$ for $t = 1$ ns (*1*) and $t = 2$ ns (*2*); (b) Density and thermal energies as functions of time.

ing was $(2-3)\times10^6$ cm s^{-1}. Calculations showed that the point exploded somewhat later for $b = 10^9$ A s^{-1} than for $b = 10^{10}$ A s^{-1}, namely, at $t = 15$ s. The pattern of explosion and parameters of the plasma differ but only slightly from those for $b = 10^{10}$ A s^{-1}.

Results of certain calculations may be verified by the available experimental data. First, it was shown in several methods that the velocity of cathode plasma scattering was 2×10^6 cm s^{-1} for copper. Second, measurements of various authors yield a plasma temperature of about several electronvolts in accordance with calculations. The agreement of results should be accepted to be satisfactory to within the experimental and computational errors for which difficulties of measuring parameters of plasma in small volumes for 10^{-9} s and approximate calculations are responsible.

The cited method was developed further in Ref. [56], where the explosion of an aluminium point was simulated. In Ref. [56] results were presented of two-dimensional mathematical simulation of unsteady hydrodynamic processes going on in the explosion of a micropoint at the aluminium cathode. Semiempirical wide-range models were invoked to describe thermodynamics, electric conduction, and thermal conduction in a dense plasma.

The mathematical description of the destruction of a cathode micropoint in the EEE is based on a system of two-dimensional equations of hydrodynamics which express the laws of conservation of mass, momentum, and energy with account being taken of electron and radiant thermal conductivity in the differential form.

The thermal and electric conductivity were calculated using semiempirical formulas and data from tables [57, 58]. To close the system of equations of continuum dynamics, the wide-range equation of state of aluminium was used [59]. It accounts for melting, evaporation, and ionisation.

The equation of state adequately describes all the data on shockwave compression of solid and porous species in the megabar range of pressure, results of experiments on isentropic relief of shock-compressed aluminium, and experimental information on thermophysical properties of metals at low pressure. The semiempirical equation of state also invokes results of quantum-mechanical calculations by the zone method and has correct asymptotics to the data of theoretical models of Thomas and Fermi, and Debye and Huckel for pressures and temperatures typical in experiments.

The system of equations was solved in the cylindrical system of coordinates on a uniform Euler mesh by the method of large particles [60]. The computational method is accurate to the first order with artificial viscosity. It is reasonably accurate and stable for large deformation flows. It was modified to compute the motion of a medium with a free surface; the computational technique and the boundary conditions are very similar to those in Ref. [61].

The heat conduction equation was solved by the local iteration method [62]. The electric explosion of an aluminium point was calculated. In calculations, the radius was assumed to be $r_0 = 2 \times 10^{-5}$ cm, the cone angle was $\theta = 12°$, and the height was $h = 1.6 \times 10^{-4}$ cm. It was presumed that the joint current increased in accordance with the linear law $i = a + bt$, with $a = 1.25$ A and $b = 10^{10}$ A s^{-1} in the explosion of the point.

Despite the simplifications made, the results of calculations satisfactorily reflect the basic physical quantities describing the electric explosion of a micropoint. The comparison of computed and experimental data verifies that the process of interest is well described in the cited approach. For example, the rate of destruction of the point is 10^5 cm s^{-1}, the velocity of the plasma scattering is 10^6 cm s^{-1}, the pressure of plasma in the crater is 10^4 at the point, and the plasma temperature is 3.5 eV.

5.3 Two-fluid hydrodynamic model

Microexplosions at points were considered above. There was no model for an ecton on a flat surface for a long time because of the difficulty of the problem. In this section, processes at a flat cathode and near it will be considered.

The heating, ablation, and scattering of the material are simulated with the unsteady hydrodynamics equations. The conducting medium in the gap, from the metal to the ideal plasma, is described by semiempirical equations of state of the material.

The geometry of an emission centre is shown in Fig. 11. It is a depression on a flat surface. The scattering of the erosion products is assumed to be spherically symmetrical. The plasma jet from the cathode scatters into a solid angle matching the opening of the circular cone.

The spherical surfaces of radii r_0' and r_0 have equal areas, and all parameters of material have the same values on these surfaces. The radius of the erosion depression increases owing to the destruction of the cathode. The radius of the jet base r_0' also increases.

The problem is one-dimensional. This facilitates calculations significantly. However, the applicability of such a model is restricted. The system of equations of two-fluid (electrons and ions with the charge $\bar{z}$) two-temperature hydrodynamics is used. These equations are written in the 8-momentum approximation [63].

The particle fluxes and associated energy fluxes between the side surface of the plasma jet and the cathode were taken into account: electron emission from a hot cathode; emission from the plasma to the cathode owing to the high temperature of electrons in the jet and a relatively low potential barrier between the side surface of the jet and the cathode; and electron emission from plasma to cathode. These fluxes were included in equations as sources of

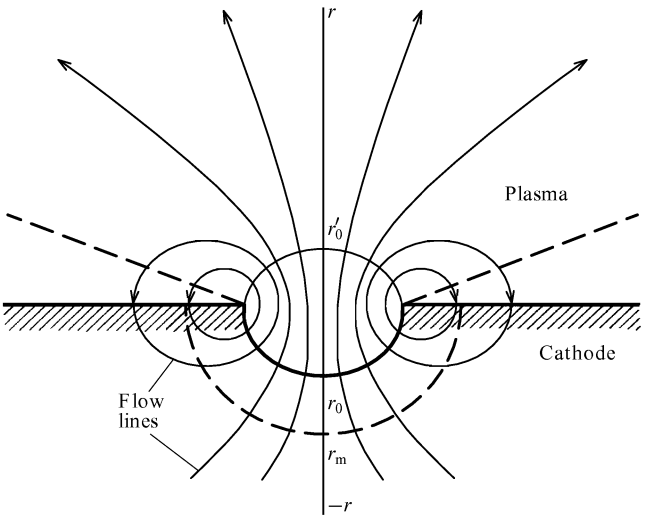

Figure 11. Geometry of the emission centre at a flat cathode.

particles and energy individually for the cathode and plasma. Ionisation losses in plasma were also taken into account.

Interpolated equations of state [65] were used to describe the material in the transient state from metal to plasma in Ref. [64]. The model was used to describe the one-phase as well as the two-phase (fluid plus vapour) states of material.

In the transient metal–plasma state, the expressions of Ref. [66] were used for the specific resistance κ and the thermal conductivity λ. First, processes at the metal–plasma interface were considered. The problem was formulated as follows.

At $t = 0$ the prescribed current began to flow through the crater of radius 10^{-5} cm. The surface of the cathode was heated to a high temperature, the pressure increased to 10^5 near the surface, the compression wave built up and propagated from the cathode with the initial velocity close to the velocity of sound $(1-2)\times10^5$ cm s^{-1}, and the erosion products scattered in the opposite direction. The point was fixed to the cross-section in which the hydrodynamic velocity of the heavy particles was zero, i.e. it was placed at the front which separates the wave from the ongoing rarefaction wave.

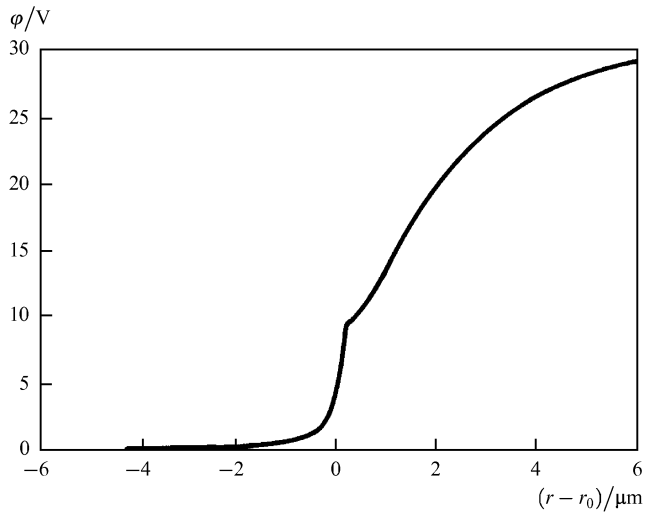

Figure 12. Distribution of potential in the transient metal–plasma region at $t = 1$ ns.

In Figs 12 and 13 certain parameters of material are presented at time $t = 1$ ns in the transient metal–plasma state for a copper cathode. By this time $r_0 \approx 1.5 \times 10^{-4}$ cm, the current density is $j \approx 3.5 \times 10^8$ A cm^{-2} (for the current 50 A).

An important result (Fig. 13) is the relatively low (10^5 V cm^{-1}) average electric field in the transient metal–plasma region. Therefore, an ecton is a thermionic process enhanced by the electric field. Evaluations show that this model is applicable only for the time $t \leqslant 10^{-9}$ s. For longer times the fluid begins to flow; this is not considered in the model.

At the initial stage of the cycle, the erosion rate is high, the ratio of the electron flux in the jet to the flux of heavy particles is 1, whereas it is on average 10–20 over the cycle. At the initial stage of the cycle, the dependence $r_0(t)$ agrees well with that in the classical thermal model. When the flux of heavy particles is small, the plasma near the cathode is weakly heated; also the ionisation rate is 1 and the velocity of ions is $(8-10)\times10^5$ cm s^{-1}.

The temperature of the plasma, its ionisation rate, and its velocity of scattering increase as the flux of heavy particles increases. The drop in potential does not exceed 30 V in the entire region between the cathode and plasma jet in spite of the high current density (10^8 A cm^{-2}).

The analysis of the plasma jet yielded interesting results. In the model, the jet was assumed to be isotropic (Fig. 13). The processes in the jet were described by the system of equations of unsteady multifluid hydrodynamics (electrons; neutrals; single, double, triple, and quadruple ions).

Ionisation and recombination were written in the Born approximation; electron impact ionisation and triple recombination were taken into account. The plasma was considered to be quasineutral; the electric field and potential were found from the equation of motion of electrons (the generalised Ohm's law).

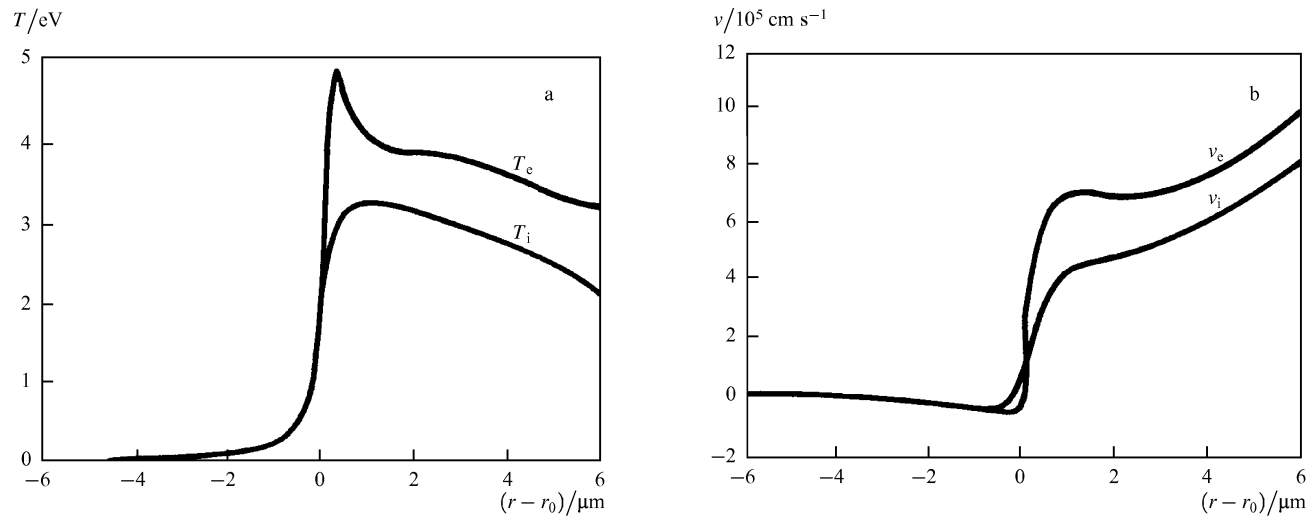

Figure 13. The parameters of copper in the transient metal–plasma region at $t = 1$ ns: (a) electron and ion temperature distributions; (b) electron and ion velocity distributions.

One of the most interesting results is the existence of a strong inverse current of thermal electrons at the periphery of the ecton zone. The voltage dropped mainly across the plasma near the cathode. The plasma potential cannot increase stepwise according to the generalised Ohm's law. Therefore there exists a fairly extended region of growth (a few micrometers) within which a relatively large number of electrons with high thermal velocities overcome the potential barrier and reach the cathode from the side surface of the jet. This inverse current can be closed only through the main emission zone at the cathode. Thus, it generates ring (toroidal) currents in the neighbourhood of the ecton. Only a part of the emission current reaches the anode; the other part circulates at the periphery of the ecton, as is shown schematically in Fig. 12.

The contribution of the cyclic current in the joint emission current depends on the size of the jet base; the electromotive force, related to the pressure gradient, increases on a decrease in r_0, and an increase in the cyclic current results. The behaviour of the potential does not change perceptibly near the cathode. The growth of the cyclic current is mainly provided for by an increase in the electron temperature near the cathode since the current density increases there.

Ions are accelerated by the pressure gradient across the plasma, for which electrons are mainly responsible. Ions are accelerated mainly within 10^{-3} cm from the cathode. At the initial stage of the cycle, the jet consists predominantly of singly charged ions.

Towards the end of the cycle, the velocity of the jet and the fraction of multiply charged ions increase also. The velocity of the jet is 1.8×10^6 cm s^{-1} at the distance 10^{-3} cm. It was shown in Ref. [64] that the ion temperature in the jet is well below the electron temperature. The electron temperature does not exceed 5 eV near the cathode.

6. Role of ectons in electric charges

6.1 Discharge in vacuum

Ectons play an important part in electric discharges in vacuum and gas. A vacuum discharge includes a vacuum breakdown, a vacuum spark, and a vacuum arc. The study of a vacuum breakdown, i.e. of loss of vacuum isolation, illustrates the mechanism in which the ecton is initiated. The vacuum spark shows the working of an ecton in unsteady conditions and of the vacuum arc in steady conditions.

6.6.1 Vacuum breakdown

I shall not discuss the diverse details of the vacuum discharge. Their descriptions may be found in Refs [4, 5, 22]. I shall only point to some of the mechanisms underlying the physical process.

(1) The FE current, flowing through a micropoint at the cathode, causes the point to heat up rapidly and explode. The associated explosive electron emission and ectons trigger a vacuum discharge [4]. On the other hand, the electrons of the FE accelerate in the vacuum gap and transfer energy to a part on the anode causing its heating, evaporation, and gas desorption from the anode.

(2) Metallic particles or impurities, bound weakly to electrodes because of the voltage applied to the gap, provide conditions for a breakdown when they hit the opposite electrode (heating and evaporation of a particle, deformation of the electrode surface, gas desorption, etc.).

(3) The surface of an electrode can change its structure under the action of the pondermotive forces of the electric field: formation of micropoints, break-off of bits of material, deformation of liquid metallic surface, etc. Then either the first or the second mechanism comes into play.

(4) Nonmetallic inclusions and films at the cathode can become efficient emission centres owing to a drop in the work function or their breakdown which plays the part of an igniting discharge.

(5) Gas desorption from electrodes encourages the gas discharge which initiates the breakdown of the vacuum gap.

Besides the cited mechanisms of initiation of a vacuum breakdown which are realisable in the presence of an applied electric field, there are methods in which electrodes are acted upon by an outer force: initiation by a plasma beam, impact of a microparticle on the cathode, auxiliary discharge over the dielectric, rapid heating of the electrode, laser radiation, etc.

In my opinion all these mechanisms, including stimulated initiation, may eventually be reduced to the energy concentration in a microvolume at the cathode, the explosion of this microvolume, and the formation of an ecton. Moreover, the mechanisms of initiation of an ecton are the same as those considered in Section 3.

6.1.2 Vacuum spark

Properties of ectons and explosive electron emission (EEE) in unsteady conditions are very pronounced in a vacuum spark. The role of EEE in a vacuum spark was identified in three series of experiments with the use of high-voltage nanosecond pulses [4]. First, the study of electron current at the initial stage of a vacuum arc. Second, the study of the glow at the cathode and anode by an image converter with nanosecond exposure time and light amplification by a factor of 10^6. Third, the study of the erosion of the cathode and anode and also the measurements of the mass carried away from their surfaces. Let us consider these results in detail.

All studies were performed with a pulse nanosecond generator. The current builds up in two stages [4]: the discharge delay time t_d and the commutation time t_c. The time t_c is typically measured between the levels 0.1 and 0.9 from the amplitude value of the current equal to U_0/R, where U_0 is the voltage amplitude and R is the discharge circuit resistance. In experiments, electrodes made of copper, aluminium, tungsten, molybdenum, steel, lead, and graphite were studied for the gap length in the range $d = 0.1 - 1$ mm [4].

The following conclusions were made about the time t_c for flat electrodes. The commutation time grows linearly with the gap length and is independent of the amplitude of the voltage applied. The current growth rate decreases on an increase in the gap length and increases on an increase in voltage. The ratio di/dt is about $d/t_c \sim 10^6$ cm s^{-1} for all materials studied. It is interesting that the time t_c obeys the same laws both for a pulse discharge and for a static discharge in vacuum. As for the time t_d, it was shown to be a function of the mean field strength and is independent either of the voltage U_0 or of the gap length d.

In essence, these conclusions reflect the fundamental properties of the process of initiation of an ecton. The occurrence of an ecton is caused by microexplosions at the

cathode owing to rapid heating of micropoints at the cathode by the FE current. Therefore, relation (2.5),

$$\int_0^{t_d} j^2 \, dt = \bar{h} , \tag{6.1}$$

is true by analogy with the explosion of a conductor. Here $\bar{h}$ is the specific action and j is the density of the FE current which initiates the ecton.

If the quantity j is constant for a time t_d and the current density is specified by the formula of Fowler and Nordheim, then

$$t_d \approx \bar{h} A^{-2} E^{-4} \exp\left(-\frac{2B}{E}\right) , \tag{6.2}$$

where E is the electric field strength at the point, A and B are factors depending on the work function of the material. From Eqn (6.2) a very strong dependence $t_d(E)$ follows. Such a dependence takes place only for relatively weak fields on the surfaces of points, for which the current densities are $j \leqslant 10^8$ A cm^{-2}.

The current density is bounded for a large j by the space charge of electrons in the region adjacent to the point [36, 41] (see Section 4.1). Therefore, the time t_d is $t_d \sim E^{-3}$, which has been verified in experiments [4]. Thus, the measurement of t_d corroborated the supposition that the EEE current delay is due to the microexplosion delay at the cathode.

The laws the quantity t_c obeys may be explained by the scattering of the cathodic plasma after the explosion. Electron-optic recording of the glow at the cathode corroborated the fact that microclusters of plasma appear several nanoseconds later upon the application of voltage [2]. These microclusters which were called cathodic flares (CF) are the plasma produced in explosions of microparts on the cathode surface. Typically one or several CF occur at the cathode, depending on the overvoltage in the gap. As a rule, only one CF occurs in a static breakdown.

The velocity of a CF is about 1.6×10^6 cm s^{-1} for copper. The study of the EEE current growth showed that the current is bounded by the space charge of the electron current the CF emits. This relationship is generally written in the form

$$i = A_0 U^{3/2} F\left(\frac{vt}{d}\right) , \tag{6.3}$$

where the constant A_0 depends on the geometry of the gap, U is the voltage between the cathode and anode, v is the velocity of the cathode plasma, d is the gap length, and t is time.

The function $F(vt/d) \sim vt/d$ for one CF at the cathode with a radius $r < vt$ when $d \gg vt$. In this case, the growth rate of the current is

$$\frac{di}{dt} \approx A_0 U_0^{3/2} \frac{v}{d} = A_0 U_0^{1/2} E_0 v ,$$

at the initial stage of the EEE, where E_0 is the initial field strength in the gap. If $E_0 \approx 10^6$ V cm^{-1}, $v = 2 \times 10^6$ cm s^{-1}, $U_0 \approx 10^4$ V, and $A_0 \approx 3.7 \times 10^{-5}$ A V$^{-3/2}$, then di/dt is of the order of 1^{10} A s^{-1}, as was obtained in the experiment [2].

The fact that the commutation time t_c grows linearly with d follows immediately from formula (6.3), since $vt_c/d = \text{const}$ for a fixed current and, consequently, $t_c \propto t_d$ [4].

The research in Ref. [4] also showed that an anode flare (AF) would be initiated not long after the cathode flare. The anode flare is due to the heating of the anode by the EEE current. This fact and also the presence of a power x-ray radiation at the anode for the time for which the CF moves to the anode and the deviation of the beam in a magnetic field perpendicular to the electric field proved uniquely that the current from the cathode is electronic in nature when an ecton functions at the cathode.

6.1.3 Vacuum arc

A vacuum arc has a number of very important properties. The difference of potentials for which the arc is drawn is very low. This difference is of the order of the ionisation potential of atoms of the material out of which the cathode is made. The arc has a threshold current i_{th} below which the arc goes out. The arc has a very high current density at the cathode of order of 10^8 A cm^{-2}. The distribution of the potential difference is very inhomogeneous across the arc. The difference of potentials peaks near the cathode. It is called the cathodic drop U_c.

The space of a vacuum arc between the cathode and anode is divided into three regions. One of them is at the cathode and is visible as a bright luminous spot which moves chaotically over the surface of the cathode. This region is called the 'cathodic spot'.

Another region occupies a larger portion between the cathode and anode and is visible as a bright diffusion glow. It is characterised by a uniform electric field distribution and a relatively low pressure gradient. At the anode there is a region which was called the 'anode region'.

All peculiar features of a vacuum arc are virtually associated with the cathodic spot. The study of an arc is essentially the study of its cathodic spot of which, as noted above, the high current density and high energy density are typical.

A set of conditions ought to be satisfied for an arc to be excited in vacuum between metallic electrodes. First, a minimal difference of potentials should be maintained, the value of which amounts to U_c in short arcs. Moreover, an arc discharge will start when the discharge current exceeds the threshold value i_{th} which is different for different materials.

At present there are the following ways in which an arc can be excited [6]: the breakdown of a vacuum gap for a fixed distance between electrodes; breaking a circuit; a current passing through a semiconductor immersed in a liquid metal; transition of a glow discharge into an arc; plasma running against the cathode, etc. Not dwelling on these methods in detail I shall only remark that in the end they are reduced to the concentration of energy in a microvolume on the surface of the cathode and to the excitation of a primary ecton by the methods described in Section 4.

The cathodic spot is a small bright luminous region on the surface of a cathode through which the current flows from the cathode to the arc column. The cathode is heated near the spot to the temperature which exceeds the boiling temperature significantly.

There are two types of cathodic spots. Spots of the first type consist of separate luminous small spots which are spaced at a distance. The metal erosion rate is not large ($\gamma_m = 5 \times 10^{-7}$ g C^{-1} for copper). These spots are due to the excitation of ectons on metallic surfaces when dielectric

films and inclusions are charged by the ionic current from the approach plasma. This is true because spots of the first type exist on an unpurified cathode only.

When the cathode is throroughly purified by heating, ionic bombardment, or in any other way, spots of the second type occur. They are larger in size and consist of separate microcraters. Moreover, spots of the first type go into spots of the second type when they function for more than several hundreds of microseconds (the current is 100 A). This can be explained by the fact that the adsorbed gas, dielectric inclusions and films are removed from the surface of the cathode for this time. The specific erosion is much larger in spots of the second type (10^{-5} – 10^{-4} g C^{-1}).

Kesaev showed in Ref. [6] that the cathodic spot has separate cells in which the current does not exceed two threshold values. If the current becomes greater than this value, then certain cells die spontaneously and other cells are formed by fission of the cells which remain. The cathode spot emits plasma, vapours, and droplets of material. The appearance of a cell, its functioning and dying off comprises an arc cycle.

We shall start from the idea of Kesaev [6] that a cathodic spot consists of separate cells from which the current i_m equal to the two threshold values of the arc current i_{th}, i.e. to $i_m = 2i_{th}$, flows. The threshold values are given in Table 4.

Table 4.

Metal	Ag	Au	Al	Cu	Fe	Mo	Ti	W
i_{th}/A	1.2	1.4	1.0	1.6	1.5	1.5	2.0	1.6

An ecton is generated as a result of interaction between the jet of a melted metal and plasma. Such jets owe their existence to high pressure near a microexplosion, up to 10^4 – 10^5 atmospheres [4]. We suppose that the jet of a liquid metal forms a droplet when the current exceeds the threshold value. This droplet will cause the density of the ion current from the plasma to increase at the joint of the jet and droplet even before the separation. This results in a larger energy concentration at the joint and in the initiation of a microexplosion owing to the Joule heating of the joint [1].

We consider an arc cycle to involve two processes. The first process is the functioning of an ecton for a time t_e. The second process is associated with the ion current near the cathode for a time t_i. The ecton current flows for the time t_e and simultaneously the new jet of a fluid metal completes its formation. Then a new ecton is formed for the time t_i. Thus, the process becomes a self-maintaining one. If an ecton is generated when, as is said above, a droplet separates, then the maintenance criterion for an arc cycle can be written in the form

$$\gamma_d t_c i_m \geqslant 1 , \tag{6.4}$$

where γ_d is the number of droplets when a charge of one Coulomb flows, $t_c = t_e + t_i$ is the arc cycle duration.

Thus, let a conic jet of a liquid metal with an angle θ be produced as a result of the functioning of an arc. Then the cone generatrix length r over which a temperature T is reached is determined from the Joule model of heating for the cone. If the temperature $T = T_{ex}$ which is equivalent to the explosion of the cone is of interest, then it follows from Eqns (2.11)–(2.13) and Eqn (2.15), since $\sin(\theta/4) \approx \theta/4$, that

$$t_e \approx \frac{1}{\pi^2} \frac{i_m^2}{a^2 \bar{h} \theta^4} , \tag{6.5}$$

$$m_e = \frac{2}{3\pi^2} \frac{i_m^3 \rho}{(a\bar{h})^{3/2} \theta^4} , \tag{6.6}$$

$$\gamma_m = \frac{2}{3} \rho (1 - \alpha) \left(\frac{a}{\bar{h}} \right)^{1/2} , \tag{6.7}$$

$$\alpha = \frac{t_i}{t_c} , \tag{6.8}$$

where α is the fraction of time for which the ionic process proceeds, t_e is the time for which the ecton functions, m_e is the mass of metal carried in the time t_e, and γ_m is the specific erosion.

Studies of a vacuum discharge showed that the explosion of a micropoint is accompanied by the ejection of a cathode plasma which moves towards the anode with a velocity $v > 10^6$ cm s^{-1} [4]. This induces the current of positive ions which move towards the anode (ionic erosion). The fraction of this current in the joint arc current is equal according to Eqn (6.7) to

$$\gamma_i = \frac{2ez}{3A} \rho (1 - \alpha) \left(\frac{a}{\bar{h}} \right)^{-1/2} , \tag{6.9}$$

where z is the plasma ionisation rate, e is the charge of an electron, A is the atomic weight of the metal out of which the cathode is made, and a is the thermal conductivity.

The current density is

$$j_e = \pi \frac{a\bar{h}\theta^2}{i_m} . \tag{6.10}$$

towards the end of the functioning of an ecton. It should be stressed that in formulas (6.5) and (6.10) quantities a and $\bar{h}$ are to be used for liquid metals when the temperature T is greater than the melting temperature.

The comparison between the theory and experiment is performed for an arc with copper electrodes. In Table 5 the characteristics of melted metallic copper are presented. The value $\bar{h} = 3 \times 10^9$ A^2 s cm^{-4} corresponds to the current density $j \geqslant 10^8$ A cm^{-2} [13], the thermal conductivity is the mean value between those for the melting and boiling temperature of metal.

Table 5.

$A/10^{-22}$ g	i_{th}/A	a/cm^2 s^{-1}	$\bar{h}/10^9$ A^2 s cm^{-4}	ρ/g cm^{-3}	z	$t_c/10^{-9}$ s
1.07	1.6 [6]	0.47 [67]	3 [13]	8.9	0.55 [8]	25 [4]

The average cycle duration $t_c = 25$ ns is evaluated by the oscillations of the potential near the cathode of a copper arc for the current 4 A [6]. It was assumed that jumps of potential correspond to the ionic phase. According to Ref. [6] the ion current fraction is small at the cathode in the arc cycle, i.e. $t_i \ll t_e$ in the average (i.e. $\alpha \ll 1$). However, it proved to be difficult to obtain the exact estimate for t_i.

First, let us evaluate the ion current fraction in the arc current and the mass carried away from the cathode per

unit charge γ_m by means of formulas (6.8) and (6.9). Kimblin showed that $\gamma_i \approx 0.07 - 0.1$ for many metals [8]. In our model this value of $\gamma_i = 0.06$ may be obtained for $\alpha = 0.2$. In this case the specific mass carried away is $\gamma_m \approx 0.6 \times 10^{-4}$ g C^{-1}. The experimental data on the quantity γ_m fall in the range $(0.4-1.15)\times10^{-4}$ g C^{-1} [4, 8, 68].

For further estimates, the value of the cone angle θ is required. If α and t_c are given, then t_e may be found and θ is determined from formula (6.5). In our case $\theta \approx 0.53$. The value of θ may also be found, given the specific number of droplets γ_d the cathodic spot of the arc ejects. For example, $\gamma_d \approx 1.4 \times 10^7$ C^{-1} for silver [7]. According to Eqn (6.9) the time t_c is $t_c \approx 22$ ns for the current $i_{th} = 1.6$ A. This time coincides with the value measured from oscillations of potential. In general, on substituting Eqn (6.4) into Eqn (6.5) we have

$$\theta^4 \approx \frac{1}{\pi^2(1-\alpha)} \frac{i_m^3 \gamma_k}{a^2 \bar{h}} . \tag{6.11}$$

It follows from Eqn (6.11) that the angle $\theta = 0.54$.

Now I shall discuss the estimate for the arc current density. It is different at different instants in time. The current density is determined from the relationship $j^2 t_d = \bar{h}$ at the instant when an ecton is initiated. The explosion delay time is $t_d \approx 10^9$ A cm^{-2} since $\bar{h} \approx 10^9$ A^2 s^{-1} cm^{-4}. The current density is determined from formula (6.10) and is equal to $j \approx 2.2 \times 10^8$ A cm^{-2} at the instant when the ecton stops functioning. This conclusion was corroborated by many authors [6, 4].

However, the current density is usually evaluated by the measured radius of the crater r_c at the cathode and the current which has flown through. If the radius of the crater is evaluated from the formula $r_c = 2(at_c)^{1/2}$, then $r_c \approx 2 \times 10^{-4}$ cm. This value is similar to Daalder's result for arc currents $i < 10$ A [69]. In this case the apparent current density will be equal to $j_c = i_m/\pi r_c^2 = 2.7 \times 10^7$ A cm^{-2}. It is close to the value measured in Ref. [70] for tungsten and copper.

From the ecton mechanism of a vacuum arc, Tanberg's effect [78] can be explained. According to this effect, when an ecton functions, the cathode experiences the action of the force which tends to span the distance between the cathode and anode.

The specific force f is introduced to characterise this effect, i.e. the force per unit current:

$$f = \frac{m_e v}{2 t_e i_m} , \tag{6.12}$$

where v is the plasma velocity. According to Ref. [6] $v \approx 10^6$ cm s^{-1} for an arc [the factor of 2 in Eqn (6.12) accounts for the anisotropy in the scattering of plasma]. It follows from Eqns (6.8) and (6.12), with consideration of the quantity $m_e/t_c i_m = \gamma_m$ to be the specific erosion of the cathode, that

$$f = \frac{\gamma_m v}{2(1-\alpha)} . \tag{6.13}$$

If γ_m is taken from Eqn (6.7), then

$$f = \frac{\rho v}{3} \left(\frac{a}{\bar{h}}\right)^{1/2} . \tag{6.14}$$

Using data from Table 5, we have $f \approx 33$ dyne A^{-1}. This value is about five times greater than the experimental data given by Tanberg for the specific force f [78].

Our analysis showed that the specific erosion was about 0.15×10^{-4} g C^{-1} in Ref. [78]. This value is 3 to 6 times less than any available data for copper. To all appearances, an unpurified cathode used in Ref. [78] is responsible for this small value, i.e. the cathodic spot was of the first type for which the specific energy is much lower than for spots of the second type.

Besides conventional arc discharges in vacuum, there are the so-called unipolar arcs. Unipolar arcs are arcs on wall elements which are in contact with plasma. The source of potential for such an arc is the contact difference of potentials between the wall and plasma owing to the thermal motion of electrons in plasma. The particular interest in such arcs was aroused when they were revealed to occur in installations for thermonuclear research, in particular, in tokamaks.

Robson and Thoneman showed theoretically that arc discharges can be maintained between the wall and plasma by the difference of potentials which is determined by the plasma thermal energy [71]. In such arcs, the current proceeds to the same cathode where the cathodic spot has appeared. Therefore, the authors of Ref. [71] called this arc unipolar.

Unipolar arcs are a source of impurities in plasma in thermonuclear installations, and also cool down the primary plasma [72]. Therefore, there are many original papers about unipolar arcs and also about the interaction between the plasma and walls in thermonuclear installations. In particular, unipolar arcs were found on walls in almost all thermonuclear installations.

Unipolar arcs are also observed when an ordinary plasma interacts with a metallic surface. The plasma is produced by outer sources or by exposing the base to a laser or high-frequency synchotron radiation [73]. The interest in unipolar arcs will increase as plasmas receive wider acceptance in various research and technological installations. The research studies on unipolar arcs are reviewed in Ref. [74].

6.2 Discharge in gas

6.2.1 Deviation from the Paschen law

Ectons play an important role in various types of electric discharges in gas. The occurrence of an ecton violates the classical mechanism of a discharge. The reasons for the occurrence of an ecton are the same as in vacuum [49]: explosions of micropeaks at the cathode because of the FE current owing to an high electric field and the breakdowns of dielectric films and inclusions at the cathode owing to their charging by discharge plasma ions. On the one hand, the presence of a gas facilitates the occurrence of an ecton since there are the gas discharge plasma and dielectric films produced in chemical interaction between the gas and metal. On the other hand, a microexplosion at the cathode is not always accompanied by a rapid current growth because atoms and molecules are an obstacle in the way of electrons in the ecton.

One of the manifestations of ecton processes is the deviation from the similarity laws, especially, from the Paschen law. This law establishes a relationship between the static breakdown voltage U on one side and the pressure p

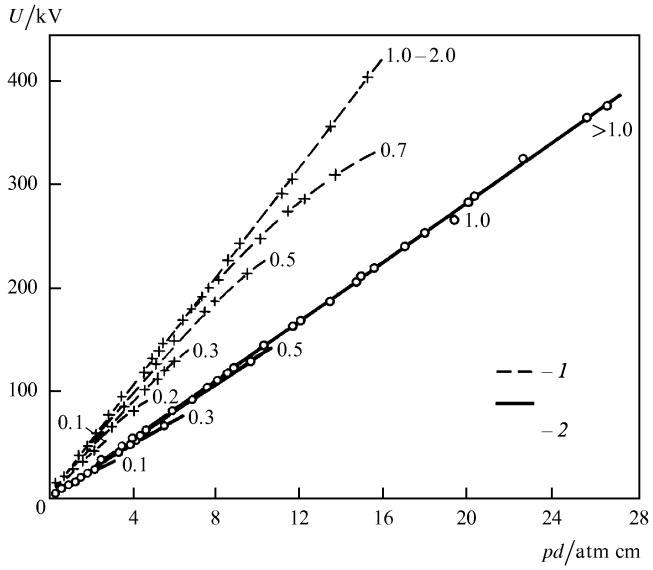

Figure 14. The right-hand branch of the Paschen curve $U = f(pd)$: (*1*) air; (*2*) hydrogen [82].

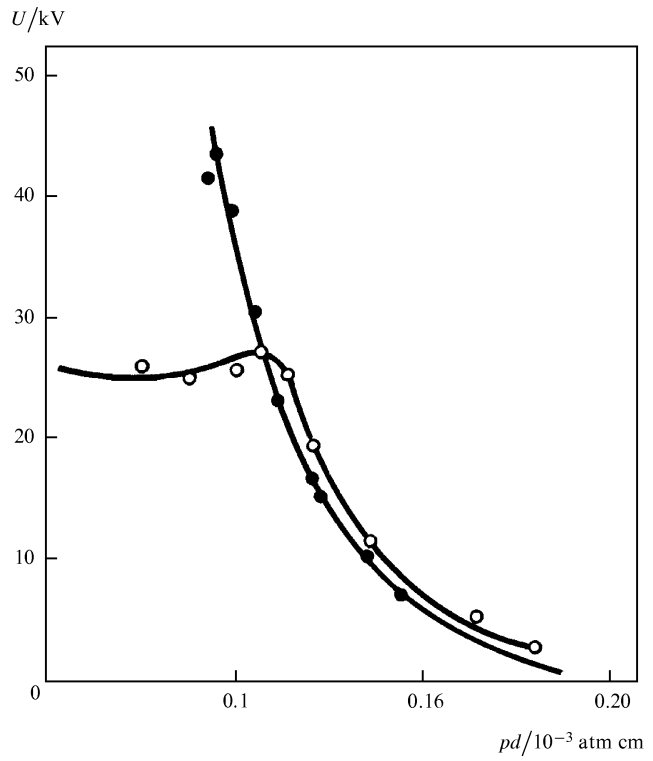

Figure 15. The left-hand branch of the Paschen curve $U = f(pd)$: (*1*) classical dependence; (*2*) dependence in the presence of an ecton [75].

and the gap length d on the other side, in the form $U = f(pd)$.

Deviations from this law are typically observed in three regions: on the right-hand side at a high pressure, on the left-hand side at a low pressure, and near the minimum. In each region, the average electric field is high over the gap (10^6 V cm^{-1} and more). Such a field induces a field emission from certain micropeaks at the cathode. Electrons will ionise the gas and ions of the ionised gas move towards

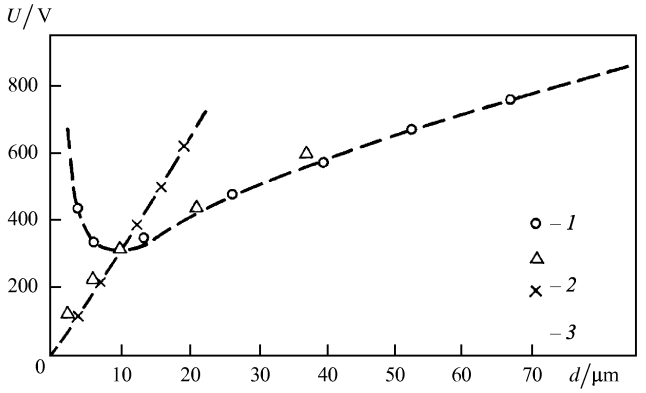

Figure 16. Neigbourhood of the minimum of the Paschen curve: (*1*) points on the Paschen curve; (*2*) points of deviation from the Paschen curve; and (*3*) points corresponding to the mean electric field 3×10^5 V cm^{-1}.

the cathode. In addition, the field emission is stimulated by the space charge of these ions. It results in further growth of the FE current density. In the end, an ecton begins to function. As is seen from Figs 14–16 all deviations from the Paschen curve result in the lower breakdown voltage in comparison with that by the Paschen law.

6.2.2 Contraction of space charges

Yet another manifestation of ecton processes in a gas discharge is the contraction of space charges, i.e. the transition of a space discharge into a channel one [75]. Examples of space discharges are a low-pressure glow discharge, a pulse self-maintained discharge which may be set up for high as well as low pressure (one atmosphere and more), and, finally, a non-self-maintained discharge with intensive external ionisation, for example, by an electron beam [76].

In such discharges, contraction begins at the cathode because of the occurrence of an ecton owing to the FE current or to the breakdown of a dielectric film at the cathode. I shall consider this effect by the example of a glowing discharge, since all discharges are contracted by the same scheme.

The distinguishing features of a glow discharge are the space current flow and the presence of a layer near the cathode across which the potential drops. Thanks to this layer, electrons from around the cathode are supplied uniformly to the discharge column. The potential drop near the cathode is typically about several hundreds of volts and the size of the region near the cathode is established to be such that the conditions are provided for a self-maintaining discharge thanks to ionisation processes in gas and secondary processes at the cathode.

Secondary electrons are generated at the cathode when it is bombarded by positive ions, because of the photoelectric effect, and because of the bombardment by fast neutral atoms produced in recharging, and in other processes. These processes provide, as a rule, for a uniform secondary electron current density at the cathode and, respectively, a uniform structure of the cathode layer.

In an ordinary glow discharge, the current density remains constant and the joint current increases since the area the discharge occupies at the cathode increases. Once the discharge has occupied the whole surface, a

further joint current growth in the circuit results in an increase in its density and in its discharge voltage. If this is the case, then it is referred to as the abnormal mode of the glow discharge. Once a specific current density is reached in the abnormal discharge, the glow discharge goes stepwise into an arc one.

The transition from a glow discharge to an arc one is accompanied by the redistribution of the current in the discharge column (the column contraction) and by the redistribution of the current at the cathode (current is localised near the cathodic spot). There are two opinions on the nature of the transition from a space discharge to an arc one.

The first opinion is that the contraction is caused by instabilities in the discharge column. For example, the column may be contracted in a glow discharge because of a larger energy release near the axis than at the periphery. As a result, the gas is heated and displaced out of the inner regions, and the density of neutral particles is reduced. In its turn, the lower density means a larger power dissapation near the discharge axis [77, 79].

There is, however, another approach, based on experimental data on the initiation of instability, which leads to contraction, near the electrodes (as a rule, near the cathode). The build-up of these instabilities is believed to initiate the instability of the discharge column. This opinion is presented less often in the literature.

Even in early experimental works, experimentalists observed both the radial contraction of the glow discharge column without changes in parameters near the cathode, and the arc formation for which the progressive instability near the cathode was responsible [81]. Moreover, the second mechanism was realisable in a wider range of experimental conditions for high and low gas pressures.

In accordance with the concept presented in this review, one of the instabilities near the cathode can appear in the case that the electric field at the cathode is sufficient for an autoemission to be initiated from certain surface parts. Then the field current will be amplified by the space charge of positive ions. This results in further current density growth, explosions of micropoints, and the initiation of an ecton.

6.2.3 Corona discharge. A corona discharge occurs typically between electrodes of the point–plane type. A high electric field (over 10^5 V cm^{-1}) occurs at the point from which the corona propagates. Depending on the polarity of the electrode of a small radius, the corona discharge is either positive or negative.

The field strength at the point is $E \approx U/r$, where r is the radius of curvature of the tip of the electrode and U is the potential at the point. The gas at the point is intensively ionised in a high field since the impact ionisation coefficient depends strongly on the electric field.

It may be concluded from data cited in Ref. [82] that, in negative coronas, effects very similar to ectons were observed under certain conditions. First, bright cathodic spots were observed at the cathode of a negative corona. Second, the authors of Ref. [82] paid special attention to depressions which appeared at the negative point in a corona discharge in nitrogen or hydrogen.

The formation of 'crater-like depressions' seemed to be very unusual since positive ions reached the cathode with the energy of no more than 1 eV. This phenomenon was observed at cathodes made of tungsten, platinum, copper, and lead. Today we can interpret this effect as an ecton.

The initiation of an ecton was observed at the initial stage of the pulse corona discharge in air in Ref. [49]. In most experiments, single rectangular pulses of controlled duration were applied to the gap of length 0.6 cm between electrodes at the initial voltage 25 kV with the edge 10^{-9} s. The radius of the point was 1 μm or more. The opposite electrode was a hemisphere of radius 0.3 cm. The surface of the point after the breakdown was viewed through a scanning electron microscope. The structure of the point was additionally monitored through a shadow electron microscope. A crater occurred independently of the polarity of the voltage applied to the point when the pulse duration was 3 ns. However, spots were initiated at points of larger radii only if the point was a cathode. In this case, erosion manifested itself in microcraters at the cathode.

Initiation of ectons at the cathode may be explained by the developing cathodic instability. The distinct nature of erosion at the cathode and anode corroborates this conclusion. The damaged surface of the cathode is covered by clustered melted balls of 1–2 μm diameter which are usually densely packed in a region of length 20–30 μm. This means that ectons are initiated, as in a vacuum discharge, in microinhomogeneities at the cathode which are present on edges of craters left from earlier breakdowns.

A cathodic spot is initiated within the time $t < 3$ ns when the polarity is negative. The current density at the anode increases as the pressure grows and it is equal, respectively, to 1.3×10^4, 2.6×10^4 and 5×10^4 A cm^{-2} for the pulse duration 20 ns and pressure 76, 152, and 228 mm Hg. Given the electron drift velocity to be $v = 10^7$ cm s^{-1}, the electron concentration is 10^{16} cm^{-3} in the widest cross-section of the diffusion channel near the anode.

6.2.4 Pseudo-spark discharge

Over the last ten years, one of the modifications of a heavy-current space discharge, a pseudo-spark, has been studied intensively [83]. The geometry of electrodes is shown in Fig. 17. This is a discharge between a hollow cathode and a hollow anode. It strikes in heavy-current commutators, which outperform thyratrons, and also in sources of electrons.

Of special interest is the emission mechanism which provides for the average current density of about 10^4 A cm^{-2}. The main characteristics of a pseudo-spark are as follows. The pressure is typically about $p \approx 0.1$ Torr in the spark gap and the gap length is $d \approx 0.1-1$ cm. The electron free path length is $\lambda_e > d$ in the gap between the electrodes.

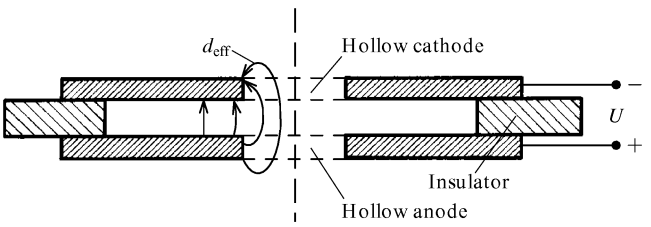

Figure 17. Principal scheme of a pseudo-spark chamber.

On initiation of a discharge in the hollow cathode, the plasma penetrates the opening and an electron beam is generated with the current up to 10–100 A. At this stage, the gas is desorbed from the surface and ionised, and the gas density amounts to 10^{16} cm^{-3} near the opening. The diameter of the glow channel is approximately equal to the diameter of the opening channel [83].

A heavy-current discharge with the current density 10^4 A cm^{-2} sets up when the plasma glows, expanding radially with the velocity 10^8 cm s^{-1}, and fills the gap between the electrodes to the extent of 5 or 6 diameters of the point. The voltage in the discharge drops to several hundreds of volts. This voltage is concentrated in a layer of thickness 10^{-4} cm and creates the field $E = (1-5) \times 10^6$ V cm^{-1} at the cathode.

Thermionic emission is considered to be the most probable explanation of the emission mechanism. The temperature of the cathode T must be greater than 3500 K for the current density to be $j = 10^4$ A cm^{-1} when $E = (2-5) \times 10^6$ V cm^{-1}. The power density must be $(3-4) \times 10^7$ W cm^{-2} for a cathode of Mo to heat the surface of the cathode to this temperature in a time $t < 50$ ns (time of initiation of a heavy-current discharge). However, even very optimistic calculations yield the power flux of no more than 10^{16} W cm^{-2}, which is clearly insufficient for heating the cathode to the melting temperature.

The microrelief of a cathode after a pseudo-spark is very similar to the relief of a cathode after an arc discharge [83]. The mass carried away from the cathode of Mo per unit charge has been measured in Ref. [83] to be equal to $(5-8) \times 10^{-5}$ g C^{-1} and is typical of an ecton. The metal is eroded mainly where the electric field is high, i.e. at the edge of the cathode (Fig. 18). Considering the nature of damage at the cathode, there are strong grounds to believe that ectons are responsible for the high average current density in a pseudo-spark.

The studies of physical processes of initiation and evolution of a vacuum discharge, and the emission mechanism in the cathodic spot of a vacuum arc and in a space gas discharge, made it possible to establish a set of laws which prove that ectons are responsible for the emission in a pseudo-spark [84]. I shall proceed from the assumption that 10^3 ectons provide for the average current density

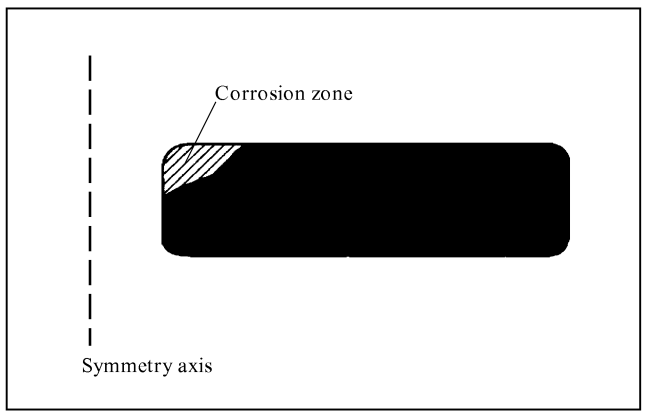

Figure 18. Schematic plan of the cathode after 5×10^6 breakdowns for the discharge duration of 90 ns and current of 20 kA [83].

10^4 A cm^{-2} in the pseudo-spark when each carries the current 10 A. The current density can amount to 10^8 A cm^{-2} in an ecton.

An ecton occurs within the time t_d provided that $j^2 t_d = \text{const}$. The time t_d is in the nanosecond range at the initial current density 10^9 A cm^{-2}. The research in Ref. [4] showed that $t_d \sim 1$ ns for a molybdenum cathode conditioned in a high vacuum when the average electric field strength is $E > 2 \times 10^6$ V cm^{-1} at the cathode. The field the space charge creates at the initial stage of a pseudo-spark is of the same order of magnitude and, consequently, it provides conditions for initiating an ecton in $t < 10$ ns.

In Ref. [83] ectons were observed at the cathode and a contracted spark was noted at the instant the current was switched on. Then, as the cathode was aged by discharges, the sparks disappeared and the discharge went into the diffusion stage. The authors made the conclusion that a super-emission occurred. This effect can be explained as follows. In the first switch-ons of current with new nonconditioned electrodes, a CF appears at the cathode for smaller fields $E \sim 10^5$ V cm^{-1} at the formation and glow stages of the beam in the region between the openings. In this case the discharge proceeds from separate areas as in a vacuum discharge.

The electric strength increases on conditioning and — as soon as the gas is spatially ionised in the gap between the electrodes, and the field is concentrated in a thin layer near the cathode in a time 2 ns — the conditions are provided for an ecton to occur spontaneously over a large area. Since the current of one ecton does not exceed, to all appearances, 10 A, the ecton plasma is stripped off and emits in the ultraviolet range [4], and the size of the spot is 0.1 mm; these cathodic spots are invisible against the background of the space glow.

The studies of eroded electrodes corroborate that the so-called superemission in pseudo-sparks is caused by ectons. The erosion is greatest at the site where the largest electric field exists, i.e. on the inner edge of the hollow cathode (Fig. 18) [83].

6.3 Processes in contacts

The surfaces of contacts are such that metals are in real contact with each other only in separate thin regions [52, 85, 86]. Even the best smooth metallic surfaces have micropeaks of 0.01–0.1 μm in height [5]. These peaks are usually on an undulating surface, the spacing of which is 10^3–10^4 μm in different conditions and the height is 1–10 μm. The roughness and undulation is the reason that two surfaces come in contact at separate points only.

When live contacts are closed, the vacuum breakdown occurs, similar to that considered above (see Fig. 16). Ectons occur as a result of explosions of micropeaks, under the action of the FE current from them. On closing the contacts, the appearing force can cause them to rebound. This force is due to the high pressure of vapours and metallic plasma as a result of microexplosions at the sites of contact.

The contacts do not move apart simultaneously when they are opened because the surface is rough. The current will flow through separate spots. Therefore, the current contraction area is melted and the melted metallic bridge is formed. The bridge, exploding, initiates an ecton. Bridges and their surfaces under the action of breaking the current are the principal issues in the physics of circuit opening.

The problem of electro-erosion machining is closely related to the issue of the functioning of contacts. It may be suggested that ectons play an important part there too. They create, for example, microjets from the cathode. These jets destroy the anode and assist in transfer of its metal to the cathode [87].

6.4 Discharge in liquid and solid dielectrics

Discharge in a fluid has been a very mysterious natural phenomenon up to the present [88]. I believe that ectons play an important part here too. The field strength amounts to 10^6 V cm^{-1} or more in the gap before the breakdown. Under such conditions, the energy may be expected to be concentrated in microvolumes at the cathode as a result of the field emission in fluid, formation of gas bubbles at the cathode and production of plasma in the bubbles, field strengthening owing to dielectric admixtures in fluid and at the cathode, etc. The probability of such a process seems to be very great when the discharge occurs in a system of the point–plane type where the point is the cathode. In such a discharge, the initial glow appears at the anode, which means probably that anode ectons are initiated.

Discharge in solid dielectrics has also been studied for a very long time. However, the mechanism of this phenomenon is as yet unclear. The electric field is also very high (10^6 V cm^{-1}) before the breakdown at the site of contact between the cathode and solid dielectric [89]. This is especially the case for discharges from point cathodes. If an ecton starts to function at the cathode, then the ejection of electrons into the dielectric and also a partial melting of the dielectric by the plasma jet are possible. This may be the initiating effect for the discharge channel in the dielectric.

The process of formation of an ecton can very vividly be illustrated by examples of discharges over the surface of a dielectric in vacuum, gas, or fluid. In this case, micropeaks at the cathode, which are in contact with the dielectric, create a tangential component of the electric field, which initiates microdischarges over the surface of the dielectric. The microexplosion current flowing through the micropeaks at the cathode causes them to explode and initiates ectons.

6.5 Abnormal ions and electrons

The idea of an ecton gives us a chance to explain a variety of effects in vacuum discharges and vacuum arcs. For example, we explained the so-called ion erosion by considering the mechanism of functioning of a vacuum arc [see formula (6.9)]. This is the motion of positive ions from cathode to anode with the velocity 10^6 cm s^{-1}. Ions acquire this energy in the emission zone when a nonideal plasma is heated by the arc current.

The idea of an ecton may be a key to the effect of the collective acceleration of ions in vacuum discharge to an energy many times greater than the voltage applied (Plyutto's effect) [90]. It is possible that electron clusters in an ecton are accelerated in unstable plasma and, capturing ions present in plasma, accelerate them.

In explosive emission, electrons are observed with an energy twice that which would be expected under applied voltage [4]. This may be explained by the example of a two-ecton mechanism. Let the current be caused initially by two ectons. One ecton disappears. The current abruptly drops by a factor of two on the disappearance of one ecton. As a result, the electromotive force of self-induction appears owing to the natural induction of the discharge circuit. This results eventually in additional acceleration of some electrons.

It is possible that by studying ectons we shall be able to explain one of the most mysterious phenomena in vacuum arcs — the so-called retrograde motion of a cathode spot [6]. The cathode spot moves in the opposite direction to the Ampere force in the crossed electric and magnetic fields. Maybe the so-called return electrons come into play, i.e. electrons which return to the cathode from the cathode plasma. The presence of such electrons is predicted by the two-fluid hydrodynamic model of an ecton (see Section 5.3). Consequently, these electrons must move in the direction opposite to the electric field. The presence of such electrons was shown in Section 4.5 in the mathematical modeling of an ecton.

7. Conclusion

Microexplosions occur when the energy (up to 10^4 J g^{-1} or more) is concentrated in microvolumes at the cathode for a short time. There are many ways in which the energy may be concentrated: Joule heating by the FE; current density amplification in microinhomogeneities at the cathode when plasma flows past them; microbreakdowns of dielectric films and embedments at the cathode in the ion current charging; laser heating of microparts at the cathode; impacts of accelerated particles on the cathode, etc. Microexplosions induce EEE. The EEE current has a peculiar structure. It consists of individual portions of electrons ($10^{11}-10^{12}$ particles) which may be compared with electron avalanches and which we call ectons. The formation time for avalanches is $10^{-9}-10^{-8}$ s.

Electrons in an ecton occur due to the rapid overheating of microparts at the cathode and this is a variation of the thermionic emission. The electron emission in an ecton stops due to the cooling of the emission zone because of thermal conduction, drop in current density, evaporation of atoms, etc.

A simple physical model of an ecton was constructed under the assumptions that the specific resistance of the metal is a function of the energy density before and after a microexplosion and that a micropart cools down solely because of thermal conduction and a drop in current density. This model is appropriate for determing the main parameters of an ecton: the number of electrons; the time for which it functions; the mass of metal carried away from the cathode; the number of ions accompanying the ecton, etc.

The ecton plays a fundamental part in electric discharges in vacuum and gas. They are responsible for initiation and evolution of a vacuum discharge and are present in each cycle of a cathodic spot in an electric arc.

The ecton approach helped to construct a relatively simple theory of a vacuum arc, which explains qualitatively and quantitatively the basic phenomena in a cathodic spot: the cyclic recurrence, mass carried away from the cathode, current density, ion erosion, Tanberg effect, etc. In my opinion, this appoach is a most fruitful one for perceiving the cathodic spot in an arc.

Ectons help to explain a number of phenomena in the physics of gas discharge: contraction of the volume of a gas discharge and its transition to an arc discharge; the deviation from the Paschen curve in a gas discharge in

the regions of the left and right branches and also near the minimum; and pulsed discharge in high electric fields.

At a low pressure, the so-called pseudo-spark discharge occurs in the region of the left branch of the Paschen curve. It is typified by a high average density of electron current from the cathode: up to 10^5 A cm^{-2} (superemission). Now it is surely established that such an emission is caused by an ecton process.

Ectons were also observed in a pulsed corona discharge. In my opinion, ectons also help to explain a number of processes in metallic contacts, in discharges in liquids, solids, dielectrics, etc. However, these assertions await additional comprehensive studies.

What are the topical issues in the near future for ectons? First, although the part of ectons in the EEE process may be regarded as established, the exact mechanism of how the emission zone of an ecton cools down is yet unclear. It seems that the interception of the current from one jet of liquid metal to another occurs.

Second, the specific actions of various metals should be measured and how they are affected by the temperature and phase state of a cathode should be established.

Third, the part of ectons in the occurrence of abnormal electrons and ions in vacuum discharges should be examined more thoroughly.

In this review I did not touch on the issue of the part played by ectons in the functioning of pulsed electrophysical devices such as high-precision electron accelerators, power pulsed x-ray devices, power relativistic microwave generators, etc. This issue is discussed in detail in the recent monograph [92]. I only want to note that the topical issue is the influence of ectons on the space–time structure of an electron beam, since this determines the quality of an electrophysical device.

References

1. Mesyats G A *Pis'ma Zh. Eksp. Teor. Fiz.* **57** (2) 88 (1993) [*JETP Lett.* **57** 95 (1993)]
2. Bugaev S P, Iskol'dskii A M, Mesyats G A, Proskurovskii D I *Zh. Tekh. Fiz.* **37** 2206 (1967) [*Sov. Phys. Tech. Phys.* **12** 1625 (1968)]
3. Mesyats G A *Issledovaniya po Generirovaniyu Nanosekundnykh Impul'sov Bol'shoi Moshchnosti* (Studies on the Generation of Powerful Nanosecond Pulses) Doctorate dissertation (Tomsk: TPI, 1966)
4. Mesyats G A, Proskurovskii D I *Impul'snyi Elektricheskii Razryad v Vakuume* (Pulse Electric Discharge in Vacuum) (Novosibirsk: Nauka, 1984)
5. Rakhovskii V I *Fizicheskie Osnovy Kommutatsii Elektricheskogo Toka v Vakuume* (Physical Foundations of Commutation of Electric Current in Vacuum) (Moscow: Nauka, 1970).
6. Kesaev I G *Katodnye Protsessy Elektricheskoi Dugi* (Processes at the Cathode in an Electric Arc) (Moscow: Nauka, 1968)
7. Utsumi T, English J H *J. Appl. Phys.* **46** (1) 126 (1975)
8. Kimblin C W *J. Appl. Phys.* **44** (7) 3074 (1973)
9. Juttner B *IEEE Trans. on Plasma Sci.* **15** (5) 474 (1987)
10. Burtsev V A, Kalinin N V, Luchinskii A V *Elektricheskii Vzryv Provodnikov* (Electrical Explosion of Conductors) (Moscow: Energoatomizdat, 1990)
11. Fortov V E, Yakubov I T *Neideal'naya Plazma* (Nonideal Plasma) (Moscow: Energoatomizdat, 1994)
12. Kvartskhava I F, Plyutto A A, Chernov F P, Bondarenko V V *Zh. Eksp. Teor. Fiz.* **30** (1) 42 (1956) [*Sov. Phys. JETP* **3** 40 (1956)]
13. Sedoi V S, Chemezova L I, Chernov A A, Kotov Yu A, Samatov O M *Megagauss Fields and Pulsed Power Systems* (New York: Nova Science, 1990)
14. Mesyats V G *Pis'ma Zh. Tekh. Fiz.* **16** (14) 30 (1990) [*Sov. Tech. Phys. Lett.* **16** 533 (1990)]
15. West R C (Ed.) *Handbook of Chemistry and Physics* (Florida: CRC Press, 1989)
16. Zel'dovich Ya B, Raizer Yu P *Fizika Udarnykh Voln i Vysokotemperaturnykh Gidrodinamicheskikh Yavlenii* (Physics of Shock Waves and High-Temperature Hydrodynamic Phenomena) (Moscow: Nauka, 1966)
17. Vitkovitsky I M *High Power Switching* (New York: Van Nostrand Reinhold, 1987)
18. Little R P, Whitney W T *J. Appl. Phys.* **34** (8) 2430 (1963)
19. Lozinskii Ya T *Vysokotemperaturnaya Metallografiya* (High-Temperature Metallography) (Moscow: Mashgiz, 1956)
20. Myuller E V, Tson' T T *Avtoionnaya Mikroskopiya* (Autoion Microscopy) (Moscow: Metallurgiya, 1972)
21. Shrednik K N *Proceedings of the VII International Vacuum Congress, Vienna, 1977* p. 2455
22. Slivkov I N *Protsessy pri Vysokom Napryazhenii v Vakuume* (High-Voltage Processes in Vacuum) (Moscow: Energoatomizdat, 1982)
23. Nadgornyi E M, Osip'yan Yu A, Perkas M D, Rosenberg V M *Usp. Fiz. Nauk* **67** (4) 625 (1959) [*Sov. Phys. Usp.* **2** 282 (1959)]
24. Poshekhonova T A, Nosov A A *Zh. Tekh. Fiz.* **40** 320 (1970) [*Sov. Phys. Tech. Phys.* **15** 233 (1970)]
25. Rohrbach F *Sur les Mecanismes qui Conduisent a la Formation de L'Etincelle Electrique a Tres Haute Tension* (Geneve: CERN 71-28, 1971)
26. Allen N K, Cox B M, Latham R W *J. Phys. D, Appl. Phys.* **12** (6) 969 (1979)
27. Cox B M *J. Phys. D, Appl. Phys.* **8** 2065 (1975)
28. Farrall G A, Owens M, Hudda F G *J. Appl. Phys.* **46** (2) 610 (1975)
29. Kaminski M *Atomnye i Ionnye Stolknoveniya na Poverkhnosti Metallov* (Atomic and Ionic Collisions on the Surface of Metals) translated into Russian (Moscow: Mir, 1967)
30. McDaniel I *Protsessy Stolknoveniya v Ionizovannykh Gazakh* (Collisions in Ionised Gases) translated into Russian (Moscow: Mir, 1967)
31. Vorob'ev G A, Mukhachev V A *Proboi Tonkikh Dielektricheskikh Plenok* (Breakdown of Thin Dielectric Films) (Moscow: Sov. Radio, 1977)
32. Gopra K L *Elektricheskie Yavleniya v Tonkikh Plenkakh* (Electric Phenomena in Thin Films) translated into Russian (Moscow: Mir, 1972)
33. Budenstein P P, Haues P I *J. Appl. Phys.* **38**, 2837 (1967)
34. Forlani F, Minnaja N *Phys. Status Solidi.* **4** (2) 311 (1964)
35. Bugaev S P, Litvinov E A, Mesyats G A, Proskurovskii D I *Usp. Fiz. Nauk* **115** (1) 101 (1975) [*Sov. Phys. Usp.* **18** 51 (1975)]
36. Dyke W P, Trolan J K, Martin E E, Barbour J P *Phys. Rev.* **5** (4) 1054 (1951)
37. Fursei G N *Issledovanie Avtoelektronnoi Emissii v Ekstremal'no Sil'nykh Elektricheskikh Polyakh i v Usloviyakh Perekhoda k Vakuumnoi Duge* (Study of Autoelectronic Emission in Extremely Strong Electric Fields and under Conditions of Transition to Vacuum Arc) Dissertation (Novosibirsk: IFP, 1973)
38. Tonks L *Phys. Rev.* **48** (6) 562 (1935)
39. Pranevichyus L I, Bartashyus I Yu, Iglunas V I *Izv. Vyssh. Uchebn. Zaved. Fiz.* (4) 44 (1969)
40. Gabovich M, Poritskii V *Pis'ma Zh. Eksp. Teor. Fiz.* **33** (6) 320 (1981) [*Sov. Phys. JETP* **33** 304 (1981)]
41. Elinson M I, Vasil'ev G F *Avtoelektronnaya Emissiya* (Autoelectronic Emission) (Moscow: GIFML, 1958)
42. Fursei G N, Zhukov V M, Baskin L M *Sil'notochnaya Emissionnaya Elektronika* (High-Current Emission Electronics) (Novosibirsk: Nauka, 1984)
43. Latham R V *High Vacuum Insulation: The Physical Basis* (New York: Academic Press, 1981)
44. Bugaev S P, Mesyats G A *Dokl. Akad. Nauk SSSR* **196** (2) 324 (1971) [*Sov. Phys. Dokl.* **16** 41 (1971)]

45. Mesyats G A *Generirovanie Moshchnykh Nanosekundnykh Impul'sov* (Generation of Powerful Nanosecond Pulses) (Moscow: Sov. Radio, 1974)
46. Schachter L, Ivers J D, Nation J A, Kerslick G S *J. Appl. Phys.* **73** (12) 8097 (1992)
47. Mesyats G A *Proceedings of the XVI International Symposium on Discharges and Electrical Insulation in Vacuum, Moscow–St. Petersburg, 23 May, 1994* p. 419
48. Puchkarev V F, Bochkarev M B *J. Phys. D, Appl. Phys.* **27** 1214 (1994)
49. Korolev Yu M, Mesyats G A *Avtoemissionnye i Vzryvnye Protsessy v Gazovom Razryade* (Autoemission and Explosion Processes in a Gas Discharge) (Novosibirsk: Nauka, 1982)
50. Ready J F *Effects of High-Power Laser Radiation* (New York: Academic Press, 1977)
51. Wang X J, Tsang T, Kirk H, et al. *Proceedings of the XV International Symposium on Discharges and Electrical Insulation in Vacuum, Darmstadt, 1992* p. 135
52. Merl V *Elektricheskii Kontakt* (Electric Contact) (Moscow: GEI, 1962)
53. Litvinov E A, Mesyats G A, Parfenov A G *Dokl. Akad. Nauk SSSR* **279** (4) 864 (1984) [*Sov. Phys. Dokl.* **29** 1019 (1984)]
54. Loskutov V V, Luchinskii A V, Mesyats G A *Dokl. Akad. Nauk SSSR* **271** (5) 1120 (1983) [*Sov. Phys. Dokl.* **28** 654 (1983)]
55. Webb F *Issledovanie Yavleniya Vzryva Provolochki pri Vremenakh menee 1 μs* (Study of Explosion of a Wire over Times less than 1 μs), in *Vzryvayushchiesya Provolochki* (Exploding Wires) translated into Russian (Moscow: Inostr. Liter., 1983)
56. Bushman A V, Leshkovich S P, Mesyats G A, Skvortsov V, Fortov V E *Dokl. Akad. Nauk SSSR* **312** (6) 1368 (1990) [*Sov. Phys. Dokl.* **35** 561 (1990)]
57. Basko M M *Uravneniya Odnomernoi Gidrodinamiki s Teploprovodnost'yu i Kinetikoi Termoyadernogo Goreniya* (Equations of One-Dimensional Hydrodynamics with Consideration for Heat Conduction and Kinetics of Thermonuclear Burning) Preprint ITEF, No. 145 (Moscow: ITEF, 1985)
58. Bespalov I M, Polishchuk A Ya *Metodika Rascheta Transportnykh Koeffitsientov Plazmy v Shirokom Diapazone Parametrov* (Computational Techniques for Transport Coefficients of Plasma in a Wide Range of Parameters) Preprint IVTAN, No. 1-257 (Moscow: IVTAN, 1988)
59. Bushman A V, Kanel' G I, Ni A L, Fortov V E *Teplofizika i Dinamika Kondensirovannykh Sred pri Intensivnykh Impul'snykh Vozdeistviyakh* (Heat Physics and Dynamics of Condensed Media under Intensive Pulse Action) (Chernogolovka: 1983)
60. Belotserkovskii O M, Davydov Yu M *Metod Krupnykh Chastits v Gazovoi Dinamike* (Method of Large Particles in Gas Dynamics) (Moscow: Nauka, 1982)
61. Bertholf L D, Buxton L D, Thorne B J, et al. *J. Appl. Phys.* **46** (9) 3776 (1975)
62. Zhukov V T *Chislennye Eksperimenty po Resheniyu Uravneniya Teploprovodnosti Metodom Lokal'nykh Iteratsii* (Numerical Experiments on Solution of Heat Conduction Equation by the Method of Local Iterations) Preprint IPM AN SSSR, No. 97 (Moscow: IPM, 1983)
63. Silin V P *Vvedenie v Kineticheskuyu Teoriyu Gazov* (Introduction into the Kinetic Theory of Gases) (Moscow: Nauka, 1971)
64. Parfenov A G *Nestatsionarnaya Model' Katodnykh i Prikatodnykh Protsessov v Vakuumnoi Duge* (Unsteady Model of Processes at the Cathode and Near the Cathode in a Vacuum Arc) Doctorate dissertation (Institute of Electrophysics, Ural Branch of RAS, 1992)
65. Kolgatin S N, Khachatur'yants A V *TVT* **20** (3) 447 (1982)
66. See Ref. [58]
67. Zinov'ev V E *Teplofizicheskie Svoistva Metallov pri Vysokoi Temperature* (Thermal Properties of Metals at High Temperature) (Moscow: Metallurgiya, 1989)
68. Daalder J E *J. Phys. D, Appl. Phys.* **8** 1647 (1975)
69. Daalder J E *IEEE Trans. Power Appar. Syst.* **93** 1747 (1974)
70. Puchkarev V F, Murzakaev A M *J. Phys. D, Appl. Phys.* **23** (1) 26 (1990)
71. Robson A E, Thoneman P C *Proc. Phys. Soc.* **73** 508 (1959)
72. McGracken, Scott P E *Nuclear Fusion* **19** (7) 889 (1979)
73. Shwizke F, Taylor R J *J. Nucl. Mater.* (93-94) 780 (1980)
74. Zykova N M, Nedospasov A V, Petrov V T *TVT* **21** (4) 778 (1983)
75. Korolev Yu D, Mesyats G A *Fizika Impul'snogo Proboya Gazov* (Physics of Pulsed Breakdown in Gases) (Moscow: Nauka, 1991)
76. Bychkov Yu I, Korolev Yu D, Mesyats G A *Usp. Fiz. Nauk* **126** (3) 451 (1978) [*Sov. Phys. Usp.* **21** 944 (1978)]
77. Ecker G, Kroll W, Zoller O *Phys. Fluids* **7** (12) 2001 (1964)
78. Tanberg R *Phys. Rev.* **35** 1080 (1930)
79. Jacob J, Mani S A *Appl. Phys. Lett.* **26** (2) 53 (1975)
80. Gamdling W A, Edels H *Nature (London)* **177** (9) 1090 (1956)
81. Boyle W S, Haworth F E *Phys. Rev.* **101** (3) 935 (1956)
82. Mick D, Crags D *Elektricheskii Proboi v Gazakh* (Electric Breakdown in Gases) translated into Russian (Moscow: Inostr. Lit., 1960)
83. Gundersen M A, Schaefer G *Physics and Application of Pseudosparks,* NATO ASI, Series B (New York: Plenum, 1989)
84. Mesyats G A, Puchkarev V F *Proceedings of the XV International Symposium on Discharges and Electrical Insulation in Vacuum, Darmstadt, 1992* p. 488
85. Holm R *Electric Contacts* (Stockholm, 1946)
86. Llewellyn Jones F, Jones R H *Z. Phys. B* **147** 45 (1957)
87. Zolotykh B N *O Fizicheskoi Prirode Elektroiskrovoi Obrabotki Metallov* (On the Physical Nature of Electromachining of Metals), in *Elektroiskrovaya Obrabotka Metallov* (Electromachining of Metals) (Moscow: Izd. AN SSSR, 1957) No. 1, p. 38
88. Ushakov V Ya *Impul'snyi Elektricheskii Proboi Zhidkostei* (Pulsed Electric Breakdown in Fluids) (Tomsk: Izd. TGU, 1975)
89. Vorob'ev A A, Vorob'ev G A *Elektricheskii Proboi i Razrushenie Tverdykh Dielektrikov* (Electrical Breakdown and Destruction of Solid Dielectrics) (Moscow: Vysshaya Shkola, 1966)
90. Korop E D, Plyutto A A *Zh. Tekh. Fiz.* **40** 2534 (1970) [*Sov. Phys. Tech. Phys.* **15** 1986 (1971)]
91. Razumikhin M A *Erozionnaya Ustoichivost' Malomoshchnykh Kontaktov* (Erosion Resistance of Weak contacts) (Moscow: Energiya, 1964)
92. Mesyats G A *Ektony* (Ectons) (Ekaterinburg: Nauka, 1995)